(12) INTERNATIONAL APPLICATION PUBLISHED UNDER THE PATENT COOPERATION TREATY (PCT)

(19) World Intellectual Property Organization
International Bureau

(43) International Publication Date
07 March 2024 (07.03.2024)

WIPO | PCT

(10) International Publication Number
WO 2024/047571 A1

(51) International Patent Classification:
C07F 5/02 (2006.01) *C07D 215/48* (2006.01)
C07D 473/12 (2006.01) *C07D 213/67* (2006.01)
C07D 213/79 (2006.01)

(21) International Application Number:
PCT/IB2023/058612

(22) International Filing Date:
31 August 2023 (31.08.2023)

(25) Filing Language: English

(26) Publication Language: English

(30) Priority Data:
63/403,025 01 September 2022 (01.09.2022) US

(72) Inventor; and

(71) Applicant: **SAVOI, Guilherme** [BR/AR]; Carpintero 11 Lote 341 B° Los Sauces – Nordelta - Partido de Tigre, Buenos Aires (AR).

(74) Agent: **GUERRA IP**; São Carlos, 1113, Porto Alegre (BR).

(81) Designated States *(unless otherwise indicated, for every kind of national protection available)*: AE, AG, AL, AM, AO, AT, AU, AZ, BA, BB, BG, BH, BN, BR, BW, BY, BZ, CA, CH, CL, CN, CO, CR, CU, CV, CZ, DE, DJ, DK, DM, DO, DZ, EC, EE, EG, ES, FI, GB, GD, GE, GH, GM, GT, HN, HR, HU, ID, IL, IN, IQ, IR, IS, IT, JM, JO, JP, KE, KG, KH, KN, KP, KR, KW, KZ, LA, LC, LK, LR, LS, LU, LY, MA, MD, MG, MK, MN, MU, MW, MX, MY, MZ, NA, NG, NI, NO, NZ, OM, PA, PE, PG, PH, PL, PT, QA, RO, RS, RU, RW, SA, SC, SD, SE, SG, SK, SL, ST, SV, SY, TH, TJ, TM, TN, TR, TT, TZ, UA, UG, US, UZ, VC, VN, WS, ZA, ZM, ZW.

(84) Designated States *(unless otherwise indicated, for every kind of regional protection available)*: ARIPO (BW, CV, GH, GM, KE, LR, LS, MW, MZ, NA, RW, SC, SD, SL, ST, SZ, TZ, UG, ZM, ZW), Eurasian (AM, AZ, BY, KG, KZ, RU, TJ, TM), European (AL, AT, BE, BG, CH, CY, CZ, DE, DK, EE, ES, FI, FR, GB, GR, HR, HU, IE, IS, IT, LT, LU, LV, MC, ME, MK, MT, NL, NO, PL, PT, RO, RS, SE, SI, SK, SM, TR), OAPI (BF, BJ, CF, CG, CI, CM, GA, GN, GQ, GW, KM, ML, MR, NE, SN, TD, TG).

Published:
— *with international search report (Art. 21(3))*
— *in black and white; the international application as filed contained color or greyscale and is available for download from PATENTSCOPE*

(54) Title: CRISABOROLE COCRYSTAL DERIVATIVES

Fig. 1

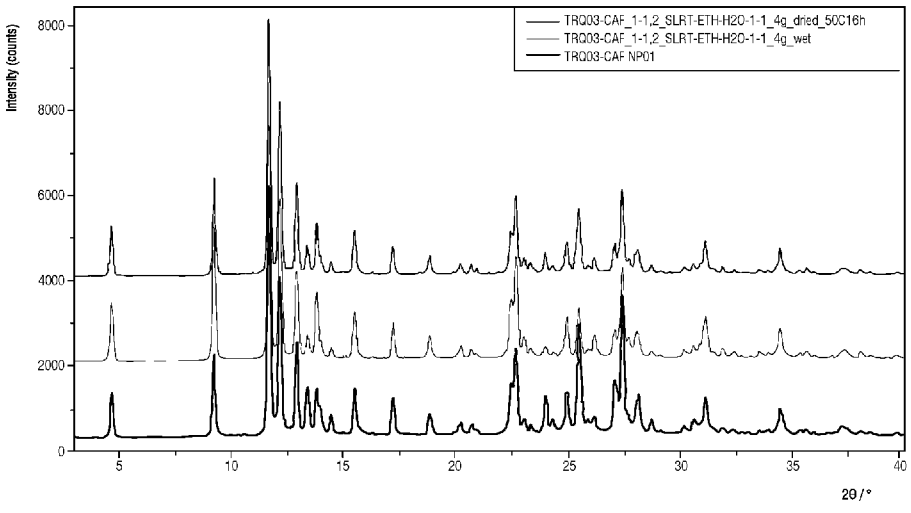

(57) Abstract: The present invention provides new co-crystal derivatives (coformers: Caffeine, Picolinic Acid, Quinaldic Acid, and Pyridoxine) of 4-((1-hydroxy-1,3- dihydrobenzo[c][1,2]oxaborol-5-yl)oxy)benzonitrile (Crisaborole) having varied dissolution when compared to free crisaborole.

WO 2024/047571 A1

CRISABOROLE COCRYSTAL DERIVATIVES

Field of the Invention

The present invention pertains to the field of pharmaceutical solid forms of Crisaborole, particularly methods of making such solid forms with varying dissolution properties and uses thereof for various medical treatments. More particularly the pharmaceutical forms are Crisaborole cocrystals obtained with caffeine, picolinic acid, quinaldic acid and pyridoxine as coformers.

Background of the Invention

The present invention refers to derivatives of 4-((1-Hydroxy-1,3-dihydrobenzo[c][1,2]oxaborol-5-yl)oxy)benzonitrile (Crisaborole). Crisaborole is a nonsteroidal topical medication used for the treatment of mild-to-moderate atopic dermatitis in adults and children. It is a phosphodiesterase 4 (PDE-4) inhibitor. PDE-4 inhibition results in increasing levels of intracellular cyclic adenosine monophosphate.

Table 1. General information of the pure drug.

Product name:	Crisaborole
Internal product code:	TRQ03
Molecular name:	4-((1-Hydroxy-1,3-dihydrobenzo[c][1,2]oxaborol-5-yl)oxy)benzonitrile
Molecular Formula:	$C_{14}H_{10}BNO_3$
Molecular Structure:	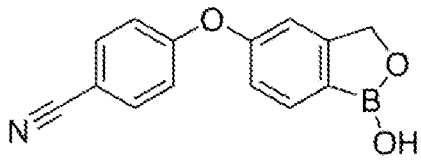
Molecular Weight	251.05
Appearance:	White powder

Three crisaborole anhydrous forms were described, named Form I, Form II and Form III. In spite of the reported data, the nature of the forms is still not clearly disclosed, and the same form is reported to be an anhydrous species

(*Cryst. Growth Des.,* 2018, *18,* 4416) and a hydrate derivative (US2021002307A1).

Moving further, several solvates were described, named Form D, Form E and Form F; finally, additional species, such as Form III (labeled as Form V) and Form IV, the nature of which was not completely disclosed, were reported in some patents.

With regard to Crisaborole cocrystals, only one example was reported in literature, with the species arising from the reaction of Crisaborole with 4,4'-Bipyridine *(Cryst. Growth Des.* 2018, *18,* 4416). No other derivatives were found in literature.

Cocrystals are crystalline molecular complexes of two or more non-volatile compounds bound together in a crystal lattice by non-ionic interactions. Pharmaceutical cocrystals are cocrystals of a therapeutic compound, e.g., an active pharmaceutical ingredient (API), and one or more non-volatile compound(s) (referred to herein as coformer). A coformer in a pharmaceutical cocrystal is typically a non-toxic pharmaceutically acceptable molecule, such as, for example, food additives, preservatives, pharmaceutical excipients, or other APIs. A cocrystal of an API is a distinct chemical composition of the API and coformer(s) and generally possesses distinct crystallographic and spectroscopic properties when compared to those of the API and coformer(s) individually. Crystallographic and spectroscopic properties of crystalline forms are typically measured by X-ray powder diffraction (XRPD) and single crystal X-ray crystallography, among other techniques. Cocrystals often also exhibit distinct thermal behavior. Thermal behavior is measured in the laboratory by such

techniques as capillary melting point, thermogravimetric analysis (TGA) and differential scanning calorimetry (DSC).

As crystalline forms, cocrystals may possess more favorable solid state, physical, chemical, pharmaceutical and/or pharmacological properties or may be easier to process than known forms or formulations of the API. For example, a cocrystal may have different dissolution and/or solubility properties than the API, and can, therefore, be more effective in therapeutic delivery. In the case of Crisaborole this may include more rapid skin permeation due to enhanced aqueous dissolution to favor formulation or alternatively a controlled slower release formulation due to reduced aqueous dissolution. The skin is a multi-complex membrane and changes from an avascular and lipophilic structure (stratum corneum) to a more aqueous structure (the viable epidermis and dermis). Uncomplicated penetration of a substance requires both solubility in the lipophilic environment and the more aqueous environment (Xenobiotica, 1987, 17, (3), 325). A cocrystal may also affect other pharmaceutical parameters such as storage stability, compressibility and density (useful in formulation and product manufacturing), permeability, and hydrophilic or lipophilic character. New pharmaceutical compositions comprising a cocrystal of a given API, therefore, may have attractive or superior properties as compared to its natural state or existing drug formulations.

For the sake of clarity and comprehension of the description, the following Table comprises a Glossary of terms used along the same.

Table 2. Glossary: Abbreviation table

Abbreviation	Definition
ACT	Acetone
API	Active Pharmaceutical Ingredient
CAF	Caffeine

DSC	Differential Scanning Calorimetry
EGA	Evolved Gas Analysis
ETA	Ethyl acetate
ETH	Ethanol
EvHT	Evaporation at High Temperature (60 °C)
EvRT	Evaporation at Room Temperature
FT-IR	Fourier Transform Infrared Spectroscopy
GR	Grinding
HT	High temperature
KN	Kneading (Liquid assisted grinding)
MET	Methanol
NMR	Nuclear Magnetic Resonance
NP	New Pattern
PIC	Picolinic acid
PYX	Pyridoxine
QNL	Quinaldic acid
RH	Relative Humidity
SL	Slurry
SLRT	Slurry at Room Temperature
SM	Starting Material (Crisaborole)
TGA	Thermal Gravimetric Analysis
TRQ03	Crisaborole
XRPD	X-Ray Powder Diffraction

Brief description of the drawings

The features and advantages of certain embodiments will be more readily appreciated when considered in conjunction with the accompanying figures. The figures are not to be construed as limiting any of the preferred embodiments.

Figure 1 is the XRPD pattern of solid TRQ03-CAF NP01 isolated from SL experiment using CAF.

Figure 2 is the ^{1}HNMR spectrum of TRQ03-CAF NP01.

Figure 3 is the FT-IR spectrum of TRQ03-CAF NP01.

Figure 4 shows the DSC profile of TRQ03-CAF NP01.

Figure 5 is the TGA profile of TRQ03-CAF NP01.

Figure 6 is the XRPD pattern of solid TRQ03-PIC NP01 isolated from SL experiment using PIC.

Figure 7 is the ^{1}HNMR spectrum of TRQ03-PIC NP01. The structures of Crisaborole and picolinic acid are included to specify some of the signals.

Figure 8 is the FT-IR spectrum of TRQ03-PIC NP01.

Figure 9 is the DSC profile of TRQ03-PIC NP01.

Figure 10 is the TGA profile of TRQ03-PIC NP01.

Figure 11 is the XRPD pattern of solid TRQ03-QNL NP01 isolated from SL experiment using QNL.

Figure 12 is the ^{1}HNMR spectrum of TRQ03-QNL NP01. The structures of Crisaborole and quinaldic acid are included to specify some of the signals.

Figure 13 is the FT-IR spectrum of TRQ03-QNL NP01.

Figure 14 is the DSC profile of TRQ03-QNL NP01.

Figure 15 is the TGA profile of TRQ03-QNL NP01.

Figure 16 is the XRPD pattern of solid TRQ03-PYX NP01 isolated from SL experiment using PYX.

Figure 17 is the ^{1}HNMR spectrum of TRQ03-PYX NP01. The structures of Crisaborole and pyridoxine are included to specify some of the signals.

Figure 18 is the FT-IR spectrum of TRQ03-PYX NP01.

Figure 19 is the TGA profile of TRQ03-PYX NP01.

Figure 20 is the DSC profile of TRQ03-PYX NP01.

Figure 21 is a comparative dissolution profile of TRQ03-CAF NP01, TRQ03-PIC NP01, TRQ03-QNL NP01, TRQ03-PYX NP01, and Crisaborole as-is.

Detailed description of the invention

Since no standardized methods and/or definite rules have been established in the prior art for assessment of physico-chemical properties of co-formers necessary for co-crystal formation (Arun Kumar et al., A Review about Regulatory Status and Recent Patents of Pharmaceutical Co-Crystals, *Adv. Pharm. Bull.*, 2018, 8(3), 355-363, doi:10.15171/apb.2018.042, http://apb.tbzmed.ac.ir, see paragraph entitled "Non-obviousness" on page 357), 30 different coformers were screened and satisfactory results were obtained with caffeine, picolinic acid, pyridoxine and quinaldic acid.

The object of the present invention is to provide new cocrystals of Crisaborole having varied dissolution properties over the pure drug, methods of making such solid forms and uses thereof for various medical treatments. In some embodiments the disease or condition is selected from: psoriasis and allergic dermatitis which are non-infectious inflammatory diseases with chronic and recurrent disease. Currently, although some treatments can be used to control these diseases, other treatments are still under investigation. Appropriate treatments can help relieve symptoms and prolong the interval. Cribboron (also known as Crisaborole, AN-2728) is a topical boron-containing anti-inflammatory compound developed by Anacor Pharmaceuticals Inc. that inhibits PDE4 activity, thereby inhibiting TNFalpha, IL-12, IL-23 and release of other cytokines. Crisaborole has a good therapeutic effect on skin diseases such as psoriasis and allergic dermatitis. It was approved by the US FDA on December 14, 2016.

EXPERIMENTAL

Preferred embodiments of the invention

In a preferred embodiment of the invention, a Crisaborole cocrystal was prepared named **TRQ03-CAF NP01** using caffeine as the coformer.

In a further preferred embodiment of the invention, a Crisaborole cocrystal was prepared named **TRQ03-PIC NP01** using picolinic acid as the coformer.

In another preferred embodiment of the invention, a Crisaborole cocrystal was prepared named **TRQ03-QNL NP01** using quinaldic acid as the coformer.

In another preferred embodiment of the invention, a Crisaborole cocrystal was prepared named **TRQ03-PYX NP01** using pyridoxine as the coformer.

Preparation and evaluation of the preferred cocrystals of the invention

1) TRQ03-CAF NP01

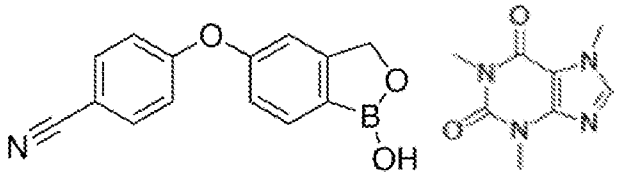

Crisaborole SM Form III Caffeine

Synthesis

Crisaborole (4 g) and 1.2 equivalents of Caffeine (3.713 g) were weighed in a 100 mL reactor vessel equipped with an anchor stirrer. Ethanol/Water 1:1 v/v mixture (80 mL) was added, and the reaction mixture was stirred at 300 rpm overnight. The almost complete dissolution of the suspended powders occurred after the solvent addition, followed by the immediate precipitation of a solid.

After approx. 16 hours, the solid was isolated by vacuum filtration using a buchner filter equipped with a 55 mm por. 42 paper filter, washed with 8 mL of solvent mixture, and dried on the filter for approx. 30 minutes. The recovery of the desired derivative was confirmed by XRPD analysis.

The isolated solid was then dried at 50°C for approx. 16 hours, and the recovery of the desired derivative was again confirmed by XRPD analysis (Figure 1). 6.714 g of TRQ03-CAF NP01 were isolated (yield = 91.0%).

The ^{1}HNMR spectrum (Figure 2) revealed the presence of Crisaborole and Caffeine in the stoichiometric ratio TRQ03 : CAF 1:1.

1H-NMR (400 MHz, DMSO-d6) δ: 9.22 (s, 1H), 8.00 (d, J1 = 0.6 Hz, 1H), 7.88-7.83 (m, 2H), 7.80 (d, J1 = 8.0 Hz, 1H), 7.18-7.13 (m, 3H), 7.10 (dd, J1 = 2.0 Hz, J2 = 8.0 Hz, 1H), 4.97 (s, 2H), 3.87 (d, J1 = 0.6 Hz, 3H), 3.40 (s, 3H), 3.21 (s, 3H).

The structural integrity of the molecule was confirmed.

FT-IR

Figure 3 shows the FT-IR spectrum of TRQ03-CAF NP01 and the peaks list can be found in the table below.

Table 3. FT-IR peak list of TRQ03-CAF NP01

Position (cm^{-1})	Intensity	Position (cm^{-1})	Intensity
421.60	46.907	1131.91	55.985
446.12	58.373	1175.90	46.455
466.57	73.180	1187.83	63.647
484.26	53.151	1219.86	40.899
519.42	67.777	1240.59	30.916
548.92	38.723	1289.41	66.532
572.25	62.941	1333.74	81.661
610.30	52.563	1361.44	40.784
623.84	44.399	1407.87	46.801
642.73	45.662	1417.98	43.879
651.08	73.873	1429.58	59.579

666.01	71.649	1455.14	50.687
724.94	71.650	1477.57	70.071
745.71	39.455	1501.01	54.446
764.13	56.511	1550.92	61.684
775.76	83.115	1572.24	75.881
805.57	79.331	1595.73	49.039
831.09	51.990	1639.37	36.526
837.54	56.835	1693.51	45.773
846.27	47.579	2225.65	74.547
853.23	58.741	2882.03	89.376
881.08	60.500	2948.47	85.555
938.61	58.818	3050.94	82.109
979.82	53.832	3080.47	79.859
1030.15	64.162	3130.07	75.331
1059.23	52.001	3463.93	82.381
1091.94	68.269		

Thermal analysis (DSC and TGA)

The DSC profile (Figure 4) showed a broad endothermic event at 86.5°C (Onset 71.6°C).

From TG-EG analysis (Figure 5) a weight loss of 4.3% w/w was observed in correspondence to the event recorded by DSC. The nature of the gas evolved during the TG analysis was disclosed by means of combined EG analysis. No evolution of organic solvent was detected in correspondence to the observed weight loss, so the presence of water could be assumed. The observed weight loss was compatible with the recovery of a monohydrate derivative.

Based on this observation, the observed DSC event could be ascribed to simple dehydration and amorphization, since no other events were highlighted before sample decomposition, which occurred above approx. 240°C.

2) TRQ03-PIC NP01

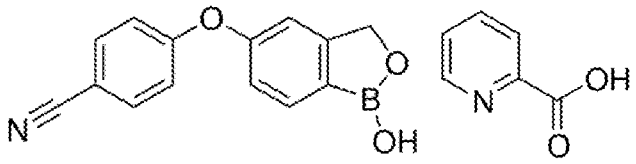

Crisaborole SM Form III Picolinic acid

Synthesis

Crisaborole (4 g) and 1.2 equivalents of picolinic acid (2.354 g) were weighed in a 100 mL reactor vessel equipped with an anchor stirrer. Methanol (80 mL) was added, and the reaction mixture was stirred at 300 rpm overnight. The almost complete dissolution of the suspended powders occurred after the solvent addition, followed by the immediate precipitation of a solid.

After approx. 16 hours, the solid was isolated by vacuum filtration using a buchner filter equipped with a 55 mm por. 42 paper filter, washed with 8 mL of solvent, and dried on the filter for approx. 15 minutes. The recovery of the desired derivative was confirmed by XRPD analysis.

The isolated solid was then dried at 50°C for approx. 16 hours, and the recovery of the desired derivative was again confirmed by XRPD analysis (Figure 6). 4.946 g of TRQ03-PIC NP01 were isolated (yield = 83.0%).

The ^{1}HNMR spectrum (Figure 7) revealed the presence of two species in solution, probably in equilibrium between each other.

This evidence is corroborated by the split of the signals at approx. 5 ppm, ascribable to the (Ph)-CH_2-O(B) group. As can be seen, in the described region of the spectrum, both a singlet and a double doublet were observed: the singlet

is related to the Crisaborole molecule “as-is”, while the “dd” signal could be tentatively ascribed to a species in which the B atom of Crisaborole is somehow coordinated with the N atom of the pyridine ring of Picolinic Acid, thus leading to the formation of a structure in which the H atoms of the CH_2 group are diastereotopic.

Because of this evidence, an unambiguous assignment of the signals, especially in the aromatic region, could not be done, and the stoichiometric ratio between the components of the species was calculated considering the integral of all the signals. For this reason, a value of 2 was assigned to the integral in the region 5.2-4.9 ppm, and the aromatic protons were observed to be 11.

Based on this data, the stoichiometric ratio TRQ03 : PIC was calculated as 1:1.

FT-IR

Figure 8 shows the FT-IR spectrum of TRQ03-PIC NP01 and the peaks list can be found in the table below.

Table 4. FT-IR peak list of TRQ03-PIC NP01

Position (cm^{-1})	Intensity	Position (cm^{-1})	Intensity
422.03	79.482	1189.20	77.775
430.55	82.621	1231.35	48.644
447.30	83.736	1245.62	40.356
456.79	85.456	1269.62	77.374
474.76	81.555	1287.63	85.346
492.38	80.090	1298.64	77.846
514.69	63.262	1311.85	91.835
549.27	44.491	1339.85	71.165
561.64	79.239	1346.42	71.796

573.29	70.065	1374.72	94.186
626.74	75.954	1417.60	81.268
645.54	64.569	1462.93	69.950
685.82	36.088	1474.30	76.234
699.50	70.781	1489.59	66.763
716.47	84.682	1503.51	59.931
738.13	80.974	1577.43	82.187
772.32	33.163	1598.13	59.369
783.67	69.728	1629.77	86.919
816.26	66.993	1702.59	85.764
828.36	56.301	1743.81	44.600
838.79	43.158	1979.58	94.837
845.76	48.614	2161.90	94.513
875.18	48.441	2227.86	70.710
890.27	63.834	2285.98	94.805
902.32	76.184	2323.73	94.051
944.96	46.378	2464.39	94.390
957.69	37.527	2678.41	93.709
974.75	57.653	2783.44	93.049
994.46	68.922	2859.78	85.644
1011.94	77.709	2904.96	90.867
1064.93	27.768	2943.96	92.005
1095.63	52.970	3046.43	85.721
1133.32	70.291	3078.39	86.370
1161.98	50.393	3131.08	90.400
1168.63	51.430	3478.52	92.778

Thermal analysis (DSC and TGA)

The DSC profile (Figure 9) showed a sharp endothermic event at 244.5°C (Onset 242.5°C), ascribable to sample melting and decomposition.

TG-EG analysis (Figure 10) confirmed the recovery of an anhydrous compound, since no weight loss was observed before simple degradation, which occurred at approx. 260°C.

Moreover, combined TG-EG analysis confirmed the presence of picolinic acid in the isolated derivative, as massive evolution of carbon dioxide was recorded during sample decomposition along with the evolution of o-anisylcyanide, ascribable to decomposition of Crisaborole.

3) TRQ03-QNL NP01

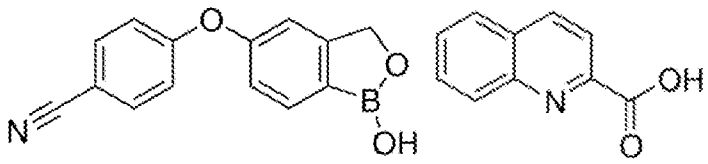

Crisaborole SM Form III Quinaldic acid

Synthesis

Crisaborole (2.5 g) and 1.2 equivalents of quinaldic acid (2.069 g) were weighed in a 100 mL reactor vessel equipped with an anchor stirrer. Methanol (50 mL) was added, and the reaction mixture was stirred at 300 rpm overnight. The almost complete dissolution of the suspended powders occurred after the solvent addition, followed by the immediate precipitation of a solid.

After approx. 16 hours, the solid was isolated by vacuum filtration using a buchner filter equipped with a 55 mm por. 42 paper filter, washed with 8 mL of solvent, and dried on the filter for approx. 15 minutes.

The isolated solid was then dried at 50 °C for approx. 16 hours, and the recovery of the desired derivative was confirmed by XRPD analysis (Figure 11). 3.564 g of TRQ03-QNL NP01 were isolated (yield = 84.4%).

From the ^{1}HNMR spectrum (Figure 12), it is possible to observe the presence of two species in solution, probably in equilibrium between each other, as already described for the TRQ03-PIC NP01 derivative.

In fact, also in this case, the split of the signals at approx. 5 ppm, ascribable to the (Ph)-CH_2-O(B) group, was observed. As can be seen, in the described region of the spectrum, both a singlet and a double doublet were found: the singlet is related to the Crisaborole molecule “as-is”, while the dd signal could be tentatively ascribed to a species in which the B atom of Crisaborole is somehow coordinated with the N atom of the pyridine ring of quinaldic acid, thus leading to the formation of a structure in which the H atoms of the CH_2 group are diastereotopic.

Because of this evidence, an unambiguous assignment of the signals, especially in the aromatic region, could not be done, and the stoichiometric ratio between the components of the species was calculated considering the integral of all the signals. For this reason, a value of 2 was assigned to the integral in the region 5.2-4.9 ppm, and the aromatic protons were observed to be 13.

Based on this data, the stoichiometric ratio TRQ03 : QNL was calculated as 1:1.

FT-IR

Figure 13 shows the FT-IR spectrum of TRQ03-QNL NP01 and the peaks list can be found in the table below.

Table 5. FT-IR peak list of TRQ03-QNL NP01

Position (cm^{-1})	Intensity	Position (cm^{-1})	Intensity
402.26	85.814	1073.43	26.242
409.35	86.297	1107.48	83.530

434.44	73.642	1136.09	73.312
451.58	60.642	1167.69	47.800
489.78	66.286	1185.56	63.816
518.85	82.352	1223.42	46.876
535.90	52.308	1244.41	28.314
548.66	50.277	1258.64	50.074
590.24	63.048	1287.57	73.661
618.03	80.908	1316.09	55.469
628.94	75.504	1339.18	84.146
656.90	82.365	1373.85	87.435
681.84	74.031	1384.34	71.383
694.74	70.009	1414.26	83.532
720.40	79.924	1464.42	62.905
729.11	81.309	1502.88	57.081
765.17	26.689	1523.89	74.111
798.06	55.992	1567.26	82.079
811.69	61.906	1580.40	80.402
821.31	62.320	1595.62	49.414
836.15	32.695	1622.57	87.054
859.49	43.813	1703.89	90.304
868.87	58.882	1745.39	26.001
912.38	56.294	2228.41	74.816
940.92	41.230	2850.77	89.572
953.26	41.380	2937.28	93.944
989.62	50.216	3086.51	92.222
1000.25	71.896	3475.71	93.817
1018.92	57.103		

Thermal analysis (DSC and TGA)

The DSC profile (Figure 14) showed a sharp endothermic event at 267.4°C (Onset 263.8°C), ascribable to sample melting and decomposition.

TG-EG analysis (Figure 15) confirmed the recovery of an anhydrous compound, since no weight loss was observed before sample degradation, which occurred at approx. 260°C.

Moreover, combined TG-EG analysis confirmed the presence of quinaldic acid in the isolated derivative as evolution of carbon dioxide was recorded during sample decomposition.

4) TRQ03-PYX NP01

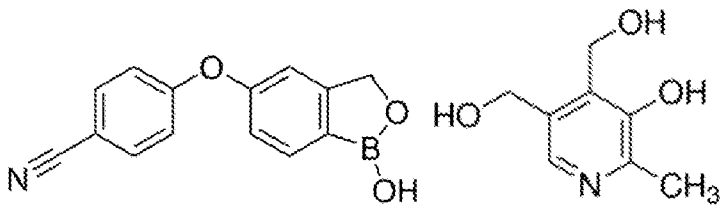

Crisaborole SM Form III Pyridoxine

Synthesis

Crisaborole (4 g) and 1.2 equivalents of pyridoxine (3.235 g) were weighed in a 100 mL reactor vessel equipped with an anchor stirrer. Methanol (80 mL) was added, and the reaction mixture was stirred at 300 rpm overnight. The almost complete dissolution of the suspended powders occurred after the solvent addition, followed by the immediate precipitation of a solid.

After approx. 16 hours, the solid was isolated by vacuum filtration using a buchner filter equipped with a 55 mm por. 42 paper filter, washed with 8 mL of solvent, and dried on the filter for approx. 30 minutes. The recovery of TRQ03-PYX NP02 (some signals shift with respect to NP01, dry sample) derivative was confirmed by XRPD analysis.

The isolated solid was then dried at 50 °C for approx. 48 hours, and the recovery of the desired TRQ03-PYX NP01 derivative was confirmed by XRPD analysis (Figure 16). 6.602 g of TRQ03-PYX NP01 were isolated (yield 94.6%).

From the ^{1}HNMR spectrum (Figure 17), it is possible to observe the presence of more species in solution in equilibrium between one another.

However, unlike what was observed for PIC and QNL derivatives, in this case the split of the signals at approx. 5 ppm could be ascribed to the pyridoxine moiety and not to the Crisaborole unit.

An equilibrium between two tautomeric forms of pyridoxine has been described in solution (J. Org. Chem. 2000, 65, 2716). As a result, both signals of the (Pyr)-CH_2-O(H) groups of pyridoxine were split into couples, thus leading to the presence of 4 signals, along with the signal of the Crisaborole (Ph)-CH_2-O(B) group.

As already described for other derivatives, because of this evidence, an unambiguous assignment of the signals, especially in the aromatic region, could not be done, and the stoichiometric ratio between the components of the species was calculated considering the integral of all the signals. For this reason, a value of 6 was assigned to the integral in the region 5.0-4.4 ppm, and the aromatic protons were observed to be 8.

Based on this data, the stoichiometric ratio TRQ03 : PYX was calculated as 1:1.

FT-IR

Figure 18 shows the FT-IR spectrum of TRQ03-PYX NP01 and the peaks list can be found in the table below.

Table 6. FT-IR peak list of TRQ03-PYX NP01

Position (cm^{-1})	Intensity	Position (cm^{-1})	Intensity
410.75	67.858	1170.67	70.095
432.16	68.981	1193.39	59.368
455.67	51.584	1226.90	48.321
491.30	73.795	1238.88	30.886
516.84	75.355	1301.85	76.761
536.33	74.947	1339.69	67.698
549.51	54.736	1365.53	78.830
568.83	64.637	1396.74	75.270
588.07	82.731	1415.28	82.297
626.58	76.866	1474.02	68.263
651.61	72.012	1497.46	69.227
662.57	71.000	1542.02	66.498
689.77	68.394	1578.94	86.249
697.49	68.010	1594.78	63.533
737.11	59.565	1609.28	90.488
780.76	61.257	1632.75	91.486
824.93	42.305	2050.16	93.713
845.77	29.736	2115.86	89.350
868.06	50.836	2161.97	90.753
881.12	74.824	2221.44	76.016
914.35	54.297	2589.24	91.609
954.05	59.190	2847.03	86.834
976.70	65.514	2877.24	91.870
997.38	67.168	2929.06	93.753
1026.19	44.369	3061.60	92.252
1068.55	65.159	3098.53	92.056
1096.32	56.287	3289.22	92.275

1114.18	81.577	3593.05	92.874
1128.81	80.705		

Thermal analysis (TGA and DSC)

TG analysis (Figure 19) recorded two consecutive weight losses partially overlapped of approx. 1.5% w/w in the region 25-100°C, and of approx. 4.2% w/w in the region 100-180°C. Nevertheless, no evolution of solvent was detected by EG analysis, suggesting the presence of water in the analyzed sample. The first weight loss could be so ascribed to the presence of imbibition water, while the second weight loss is compatible with the recovery of a monohydrated derivative.

The DSC profile (Figure 20) showed a broad endothermic event at 112.7°C (Onset 82.1°C), followed by a second small endothermic event at 169.6°C (Onset 165.0°C) and an exothermic event at 176.0°C (Onset 171.9°C).

Calorimetric events above 160°C are not well explained by comparison with TGA/EGA as a crystallization event (exo at 172°C) should not be excluded, but melting points of single components occur near that temperature region. The dehydration process was found to be a potentially critical point for stability of the derivative.

Powder dissolution results

Powder dissolution experiments were carried out in potassium phosphate buffer - pH 6.8.

The solubility of the prepared Crisaborole derivatives was evaluated through powder dissolution experiments. In a typical powder dissolution experiment, approx. 225 mg of sample were added to 600 mL of dissolution medium (pH 6.8 potassium phosphate buffer) and the resulting mixture was

stirred at 37 °C and 100 rpm. Aliquots were withdrawn from the flask at regular intervals and then injected in HPLC.

Powder dissolution experiments were carried out on Crisaborole as well as on all the scale-up derivatives, such as **TRQ03-CAF NP01, TRQ03-PIC NP01, TRQ03-PYX NP01** and **TRQ03-QNL NP01**.

Table 7 summarizes the results of powder dissolution tests conducted with TRQ03-SM and scale-up cocrystals prepared with CAF, PIC, PYX and QNL.

Table 7

Sample	2 hours		6 hours		24 hours	
	Average conc. (ppm) [SD]	Average dissolved % [SD]	Average conc. (ppm) [SD]	Average dissolved % [SD]	Average conc. (ppm) [SD]	Average dissolved % [SD]
TRQ03-SM	40.4 [4.4]	14.1 [1.1]	29.7 [2.2]	10.5 [0.5]	41.1 [1.2]	14.6 [0.3]
TRQ03-CAF NP01	40.3 [4.1]	19.0 [2.0]	30.3 [3]	14.3 [1.4]	41.4 [1.6]	19.6 [0.8]
TRQ03-PIC NP01	32.4 [4.3]	12.9 [1.7]	30.6 [2.5]	12.2 [1.0]	43.4 [2.6]	17.3 [1.0]
TRQ03-PYX NP01	36.0 [0.5]	15.2 [1.4]	36.0 [0.7]	15.2 [1.6]	35.5 [1.1]	15.0 [1.7]
TRQ03-QNL NP01	13.7 [1.3]	6.2 [0.6]	34.0 [2.5]	15.3 [1.1]	55.2 [3.7]	24.9 [1.6]

With reference to Figure 21, the following observations arise:

Crisaborole: the pure drug showed a dissolution maximum under the investigated conditions after approx. 2 hours of analysis (14.1% of powder dissolved). After this time, a decrease of the concentration of the API was observed (6 hours, 10.5% of powder dissolved), then followed by a slow increase until the final value of 14.6% of powder dissolved.

TRQ03CAF NP01: a dissolution maximum was observed after approx. 2 hours of analysis, and a value of 19.0% of powder dissolved. Moreover, after this time, a decrease of the concentration of Crisaborole was observed, with the minimum reached after approx. 6 hours (14.3% of powder dissolved) readily

followed by an apparently slight increase of the dissolved powder concentration, until a final value of 19.6% of powder dissolved.

TRQ03PIC NP01: the maximum dissolution was reached after approx. 4 hours of analysis (16.1% of powder dissolved), followed by a decrease (6 hours, 12.2% of powder dissolved) and a further increase of the amount of dissolved Crisaborole, until a final value of 17.3% of powder dissolved after 24 hours of analysis.

TRQ03PYX NP01: the dissolution profile showed 15.2% of powder dissolved after approx. 2 hours of analysis, then the concentration of Crisaborole dissolved in the medium remained almost stable at 15.0% of powder dissolved until the end of the analysis.

TRQ03-QNL NP01: the dissolution profile showed 6.2% of powder dissolved after approx. 2 hours of analysis, 15.3% after 6 hours, and the maximum value was observed at the end of the test (24.9% of powder dissolved). It is worth mentioning that this is the highest value observed within the performed experiments, suggesting that TRQ03-QNL NP01 is the most soluble species in the used medium after 24 hours.

General comments

- After 2 hours of dissolution, the caffeine derivative showed a faster dissolution rate with respect to Crisaborole as-is, even at the same order of concentration (only approx. 1.3-fold higher).

- The picolinic acid derivative showed a slower dissolution rate with respect to Crisaborole as-is (within 2 hours of analysis).

- The pyridoxine derivative showed the same dissolution kinetics as compared to Crisaborole as-is, but showed a constant profile after 2 hours of analysis.

- The quinaldic acid derivative showed the lowest dissolution kinetics with reference to Crisaborole as-is, but an apparently constant increase in time.

CLAIMS

What is claimed is:

1. Crisaborole derivative being a Crisaborole-Caffeine cocrystal, wherein Crisaborole and Caffeine are in the stoichiometric ratio of 1:1.

2. The Crisaborole derivative of claim 1, which XRPD is shown in Figure 1.

3. The Crisaborole derivative of claim 1, which DSC profile is shown in Figure 4.

4. The Crisaborole derivative of claim 1, which TGA profile is shown in Figure 5.

5. The Crisaborole derivative of claim 1, which FT-IR peak list is as follows:

Position (cm^{-1})	Intensity	Position (cm^{-1})	Intensity
421.60	46.907	1131.91	55.985
446.12	58.373	1175.90	46.455
466.57	73.180	1187.83	63.647
484.26	53.151	1219.86	40.899
519.42	67.777	1240.59	30.916
548.92	38.723	1289.41	66.532
572.25	62.941	1333.74	81.661
610.30	52.563	1361.44	40.784
623.84	44.399	1407.87	46.801
642.73	45.662	1417.98	43.879
651.08	73.873	1429.58	59.579
666.01	71.649	1455.14	50.687
724.94	71.650	1477.57	70.071
745.71	39.455	1501.01	54.446

764.13	56.511	1550.92	61.684
775.76	83.115	1572.24	75.881
805.57	79.331	1595.73	49.039
831.09	51.990	1639.37	36.526
837.54	56.835	1693.51	45.773
846.27	47.579	2225.65	74.547
853.23	58.741	2882.03	89.376
881.08	60.500	2948.47	85.555
938.61	58.818	3050.94	82.109
979.82	53.832	3080.47	79.859
1030.15	64.162	3130.07	75.331
1059.23	52.001	3463.93	82.381
1091.94	68.269		

6. The Crisaborole derivative of claim 1, which ^{1}H-NMR spectrum is shown in Figure 2.

7. Crisaborole derivative being a Crisaborole-Picolinic acid cocrystal, wherein Crisaborole and Picolinic Acid are in the stoichiometric ratio of 1:1.

8. The Crisaborole derivative of claim 7, which XRPD is shown in Figure 6.

9. The Crisaborole derivative of claim 7, which DSC profile is shown in Figure 9.

10. The Crisaborole derivative of claim 7, which TGA profile is shown in Figure 10.

11. The Crisaborole derivative of claim 7, which FT-IR peak list is as follows:

Position (cm^{-1})	Intensity	Position (cm^{-1})	Intensity
422.03	79.482	1189.20	77.775
430.55	82.621	1231.35	48.644
447.30	83.736	1245.62	40.356
456.79	85.456	1269.62	77.374
474.76	81.555	1287.63	85.346
492.38	80.090	1298.64	77.846
514.69	63.262	1311.85	91.835
549.27	44.491	1339.85	71.165
561.64	79.239	1346.42	71.796
573.29	70.065	1374.72	94.186
626.74	75.954	1417.60	81.268
645.54	64.569	1462.93	69.950
685.82	36.088	1474.30	76.234
699.50	70.781	1489.59	66.763
716.47	84.682	1503.51	59.931
738.13	80.974	1577.43	82.187
772.32	33.163	1598.13	59.369
783.67	69.728	1629.77	86.919
816.26	66.993	1702.59	85.764
828.36	56.301	1743.81	44.600
838.79	43.158	1979.58	94.837
845.76	48.614	2161.90	94.513
875.18	48.441	2227.86	70.710
890.27	63.834	2285.98	94.805
902.32	76.184	2323.73	94.051
944.96	46.378	2464.39	94.390
957.69	37.527	2678.41	93.709

974.75	57.653	2783.44	93.049
994.46	68.922	2859.78	85.644
1011.94	77.709	2904.96	90.867
1064.93	27.768	2943.96	92.005
1095.63	52.970	3046.43	85.721
1133.32	70.291	3078.39	86.370
1161.98	50.393	3131.08	90.400
1168.63	51.430	3478.52	92.778

12. The Crisaborole derivative of claim 7, which ^{1}H-NMR spectrum is shown in Figure 7.

13. Crisaborole derivative being a Crisaborole-Quinaldic acid cocrystal, wherein Crisaborole and Quinaldic Acid are in the stoichiometric ratio of 1:1.

14. The Crisaborole derivative of claim 13, which XRPD is shown in Figure 11.

15. The Crisaborole derivative of claim 13, which DSC profile is shown in Figure 14.

16. The Crisaborole derivative of claim 13, which TGA profile is shown in Figure 15.

17. The Crisaborole derivative of claim 13, which FT-IR peak list is as follows:

Position (cm^{-1})	**Intensity**	**Position (cm^{-1})**	**Intensity**
402.26	85.814	1073.43	26.242
409.35	86.297	1107.48	83.530
434.44	73.642	1136.09	73.312

451.58	60.642	1167.69	47.800
489.78	66.286	1185.56	63.816
518.85	82.352	1223.42	46.876
535.90	52.308	1244.41	28.314
548.66	50.277	1258.64	50.074
590.24	63.048	1287.57	73.661
618.03	80.908	1316.09	55.469
628.94	75.504	1339.18	84.146
656.90	82.365	1373.85	87.435
681.84	74.031	1384.34	71.383
694.74	70.009	1414.26	83.532
720.40	79.924	1464.42	62.905
729.11	81.309	1502.88	57.081
765.17	26.689	1523.89	74.111
798.06	55.992	1567.26	82.079
811.69	61.906	1580.40	80.402
821.31	62.320	1595.62	49.414
836.15	32.695	1622.57	87.054
859.49	43.813	1703.89	90.304
868.87	58.882	1745.39	26.001
912.38	56.294	2228.41	74.816
940.92	41.230	2850.77	89.572
953.26	41.380	2937.28	93.944
989.62	50.216	3086.51	92.222
1000.25	71.896	3475.71	93.817
1018.92	57.103		

18. The Crisaborole derivative of claim 13, which ^{1}H-NMR spectrum is shown in Figure 12.

19. Crisaborole derivative being a Crisaborole-Pyridoxine cocrystal, wherein Crisaborole and Pyridoxine are in the stoichiometric ratio of 1:1.

20. The Crisaborole derivative of claim 19, which XRPD is shown in Figure 16.

21. The Crisaborole derivative of claim 19, which DSC profile is shown in Figure 20.

22. The Crisaborole derivative of claim 19, which TGA profile is shown in Figure 19.

23. The Crisaborole derivative of claim 19, which FT-IR peak list is as follows:

Position (cm^{-1})	**Intensity**	**Position (cm^{-1})**	**Intensity**
410.75	67.858	1170.67	70.095
432.16	68.981	1193.39	59.368
455.67	51.584	1226.90	48.321
491.30	73.795	1238.88	30.886
516.84	75.355	1301.85	76.761
536.33	74.947	1339.69	67.698
549.51	54.736	1365.53	78.830
568.83	64.637	1396.74	75.270
588.07	82.731	1415.28	82.297
626.58	76.866	1474.02	68.263
651.61	72.012	1497.46	69.227
662.57	71.000	1542.02	66.498
689.77	68.394	1578.94	86.249
697.49	68.010	1594.78	63.533

737.11	59.565	1609.28	90.488
780.76	61.257	1632.75	91.486
824.93	42.305	2050.16	93.713
845.77	29.736	2115.86	89.350
868.06	50.836	2161.97	90.753
881.12	74.824	2221.44	76.016
914.35	54.297	2589.24	91.609
954.05	59.190	2847.03	86.834
976.70	65.514	2877.24	91.870
997.38	67.168	2929.06	93.753
1026.19	44.369	3061.60	92.252
1068.55	65.159	3098.53	92.056
1096.32	56.287	3289.22	92.275
1114.18	81.577	3593.05	92.874
1128.81	80.705		

24. The Crisaborole derivative of claim 19, which ^{1}H-NMR spectrum is shown in Figure 17.

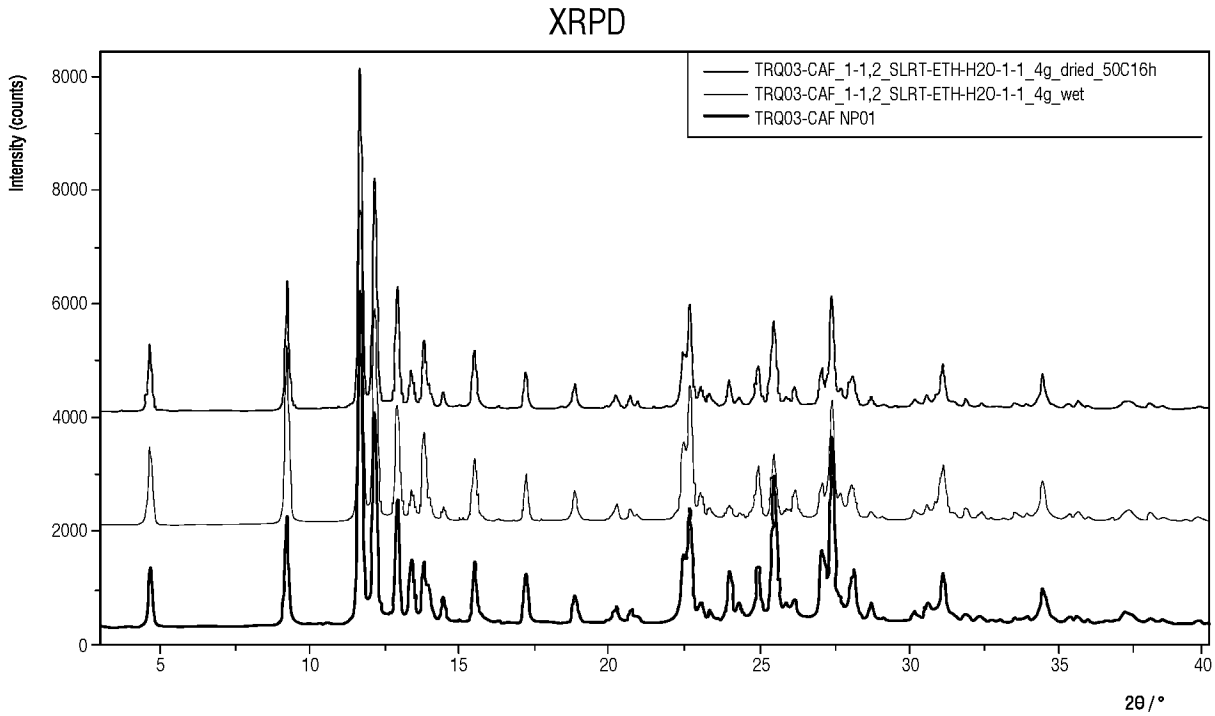
XRPD
TRQ03-CAF_1-1,2_SLRT-ETH-H2O-1-1_4g_dried_50C16h
TRQ03-CAF_1-1,2_SLRT-ETH-H2O-1-1_4g_wet
TRQ03-CAF NP01
Intensity (counts)
8000
8000
6000
4000
2000
0
5
10
15
20
25
30
35
40
2θ/°

Fig. 1

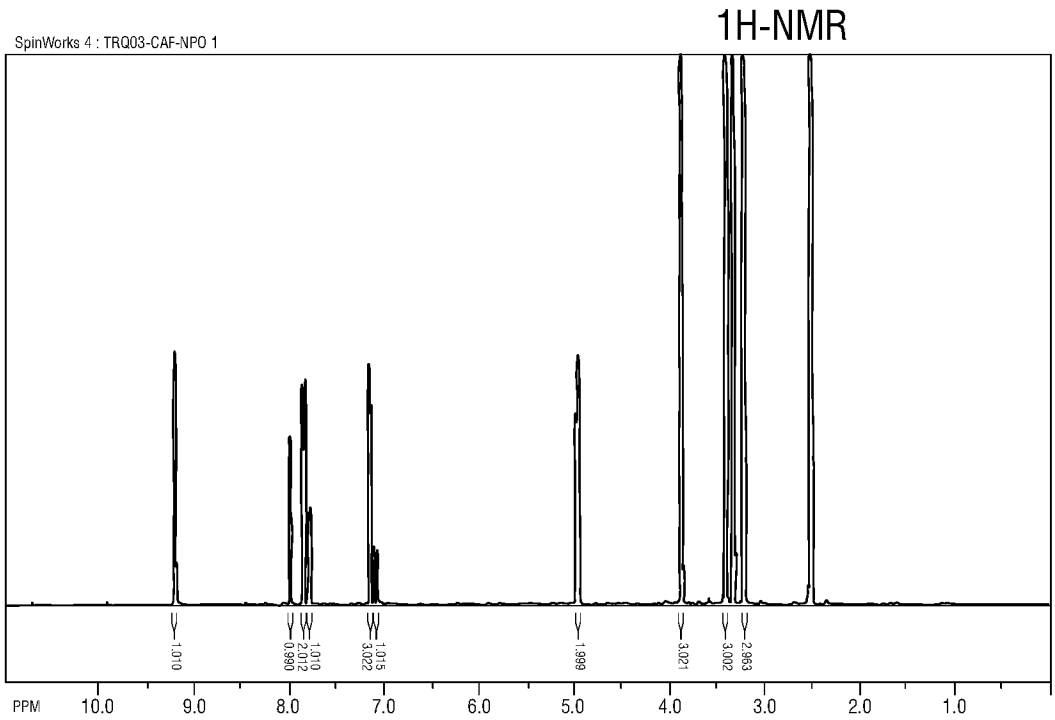
1H-NMR
SpinWorks 4 : TRQ03-CAF-NPO 1
1.010
0.990
2.012
1.010
3.022
1.015
1.999
3.021
3.002
2.983
PPM
10.0
9.0
8.0
7.0
6.0
5.0
4.0
3.0
2.0
1.0

Fig. 2

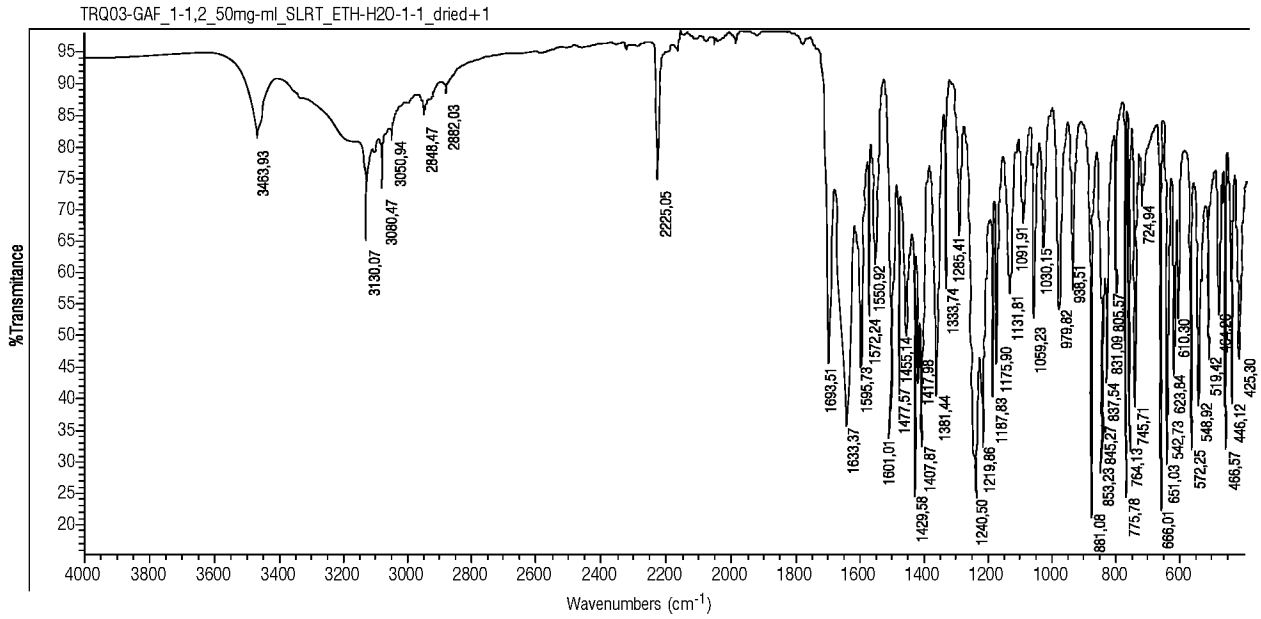
TRQ03-GAF_1-1,2_50mg-ml_SLRT_ETH-H2O-1-1_dried+1
%Transmitance
Wavenumbers (cm-1)
3463,93
3130,07
3080,47
3050,94
2848,47
2882,03
2225,05
1693,51
1633,37
1595,73
1572,24
1550,92
1601,01
1477,57
1455,14
1417,98
1429,58
1407,87
1381,44
1333,74
1285,41
1240,50
1219,86
1187,83
1175,90
1131,81
1091,91
1059,23
1030,15
979,82
938,51
881,08
853,23
845,27
837,54
831,09
805,57
775,78
764,13
745,71
724,94
666,01
651,03
642,73
623,84
610,30
572,25
548,92
519,42
466,57
446,12
425,30

Fig. 3

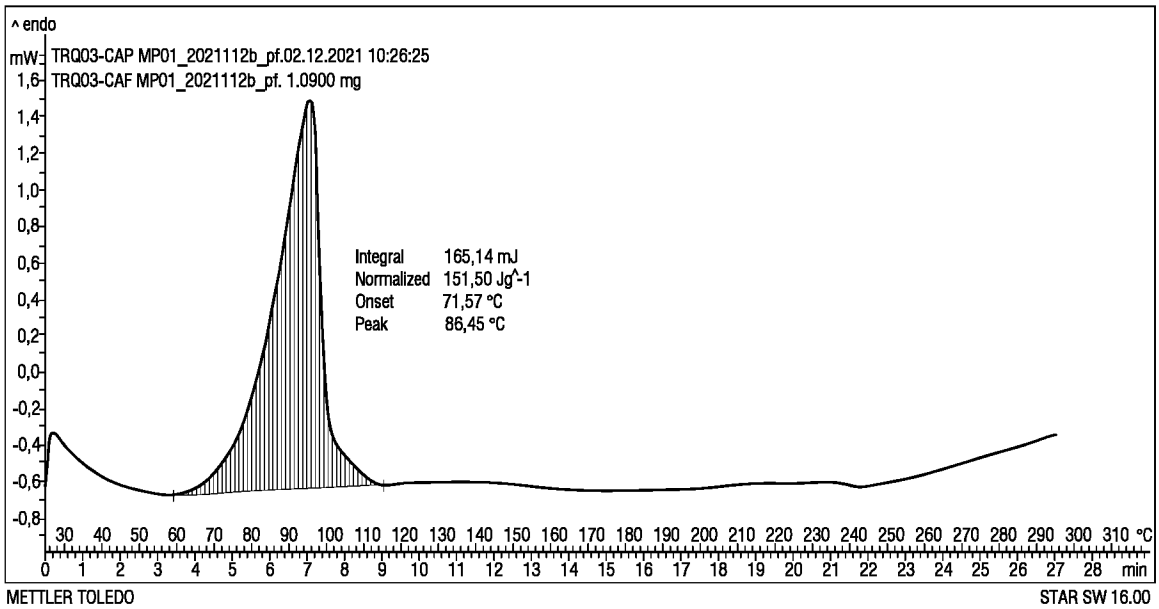
^ endo
mW
TRQ03-CAP MP01_2021112b_pf.02.12.2021 10:26:25
TRQ03-CAF MP01_2021112b_pf. 1.0900 mg
Integral 165,14 mJ
Normalized 151,50 Jg^-1
Onset 71,57 °C
Peak 86,45 °C
1,6
1,4
1,2
1,0
0,8
0,6
0,4
0,2
0,0
-0,2
-0,4
-0,6
-0,8
30 40 50 60 70 80 90 100 110 120 130 140 150 160 170 180 190 200 210 220 230 240 250 260 270 280 290 300 310 °C
0 1 2 3 4 5 6 7 8 9 10 11 12 13 14 15 16 17 18 19 20 21 22 23 24 25 26 27 28 min
METTLER TOLEDO
STAR SW 16.00

Fig. 4

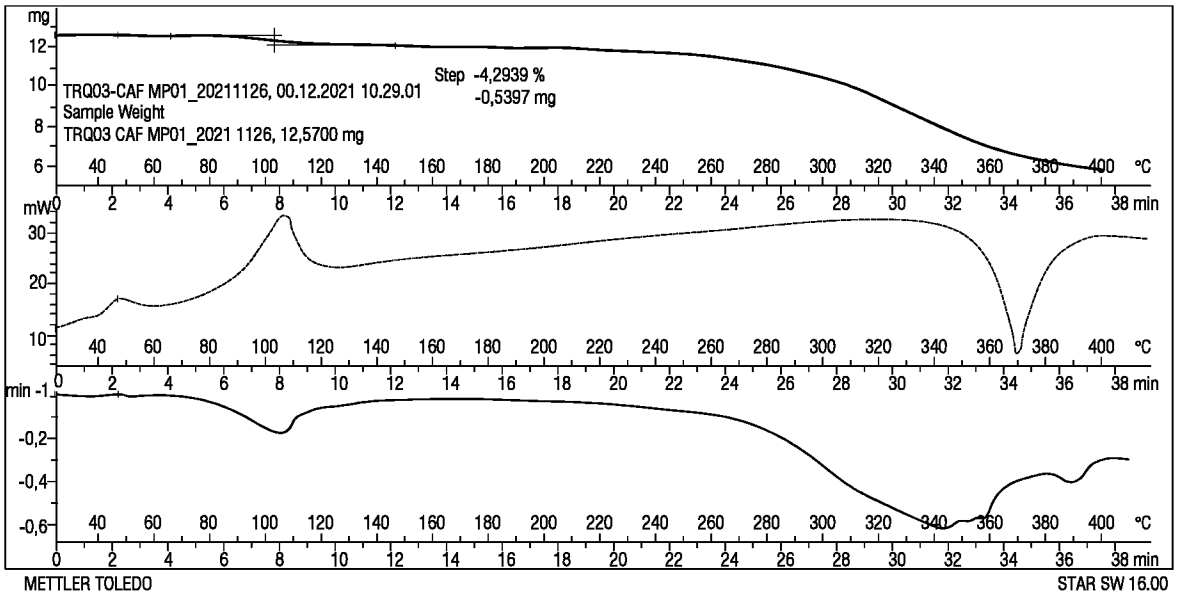
mg
12
10
8
6
TRQ03-CAF MP01_20211126, 00.12.2021 10.29.01
Sample Weight
TRQ03 CAF MP01_2021 1126, 12,5700 mg
Step -4,2939 %
-0,5397 mg
40 60 80 100 120 140 160 180 200 220 240 260 280 300 320 340 360 380 400 °C
0 2 4 6 8 10 12 14 16 18 20 22 24 26 28 30 32 34 36 38 min
mW
30
20
10
40 60 80 100 120 140 160 180 200 220 240 260 280 300 320 340 360 380 400 °C
0 2 4 6 8 10 12 14 16 18 20 22 24 26 28 30 32 34 36 38 min
min -1
-0,2
-0,4
-0,6
40 60 80 100 120 140 160 180 200 220 240 260 280 300 320 340 360 380 400 °C
0 2 4 6 8 10 12 14 16 18 20 22 24 26 28 30 32 34 36 38 min
METTLER TOLEDO
STAR SW 16.00

Fig. 5

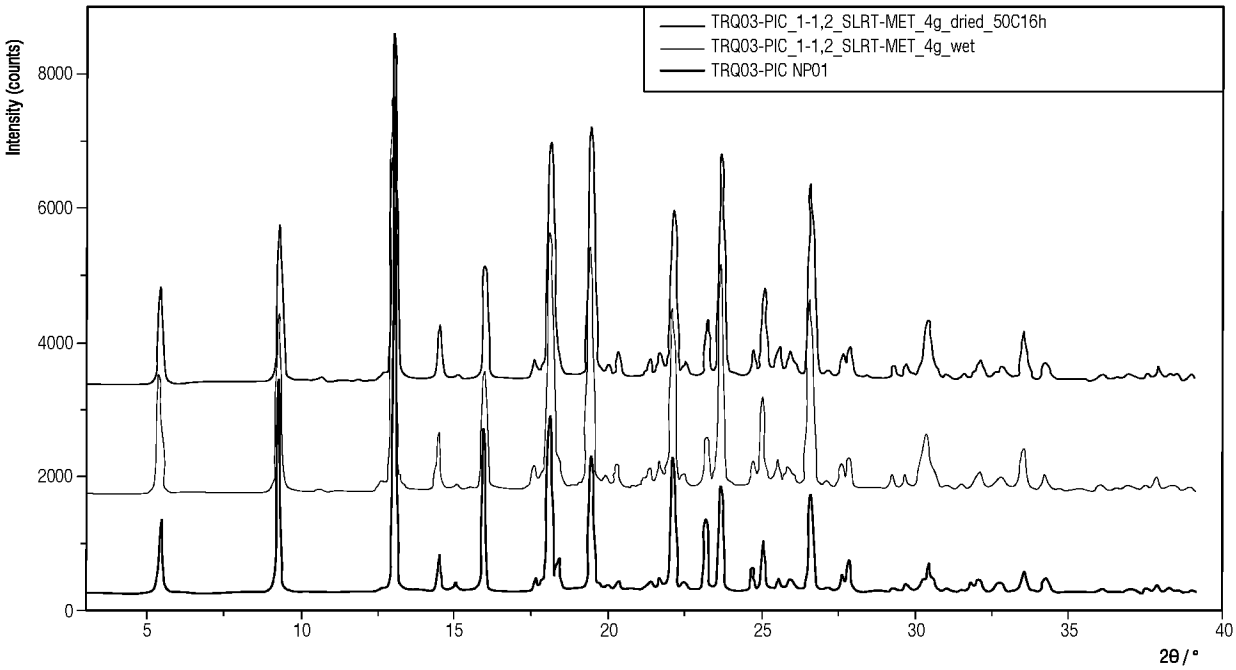
TRQ03-PIC_1-1,2_SLRT-MET_4g_dried_50C16h
TRQ03-PIC_1-1,2_SLRT-MET_4g_wet
TRQ03-PIC NP01
Intensity (counts)
8000
6000
4000
2000
0
5
10
15
20
25
30
35
40
2θ / °

Fig. 6

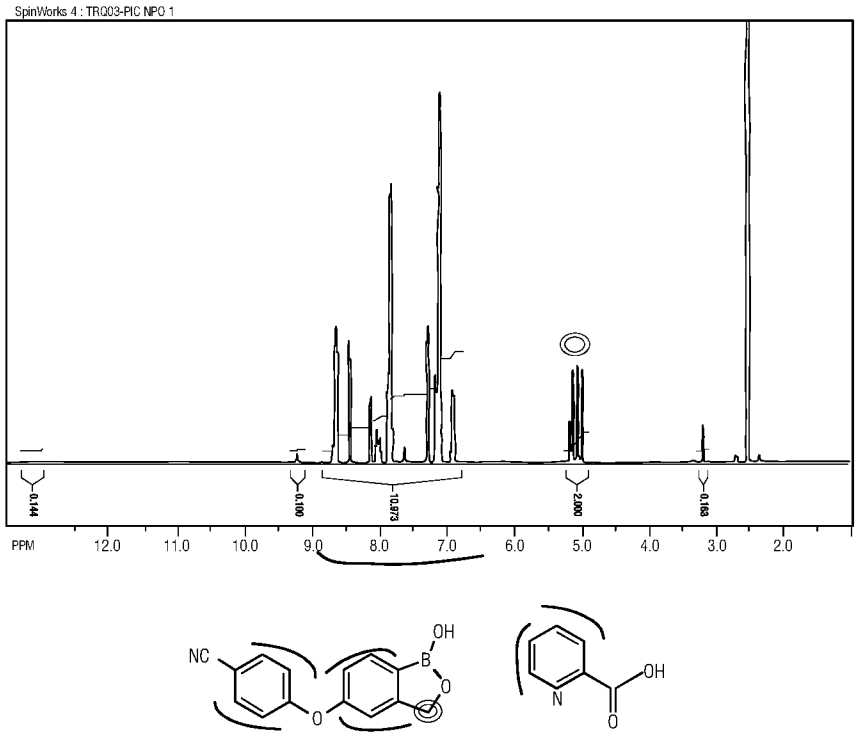
SpinWorks 4 : TRQ03-PIC NPO 1
0.144
0.100
10.973
2.000
0.183
PPM
12.0
11.0
10.0
9.0
8.0
7.0
6.0
5.0
4.0
3.0
2.0
NC
O
B
OH
O
N
OH
O

Fig. 7

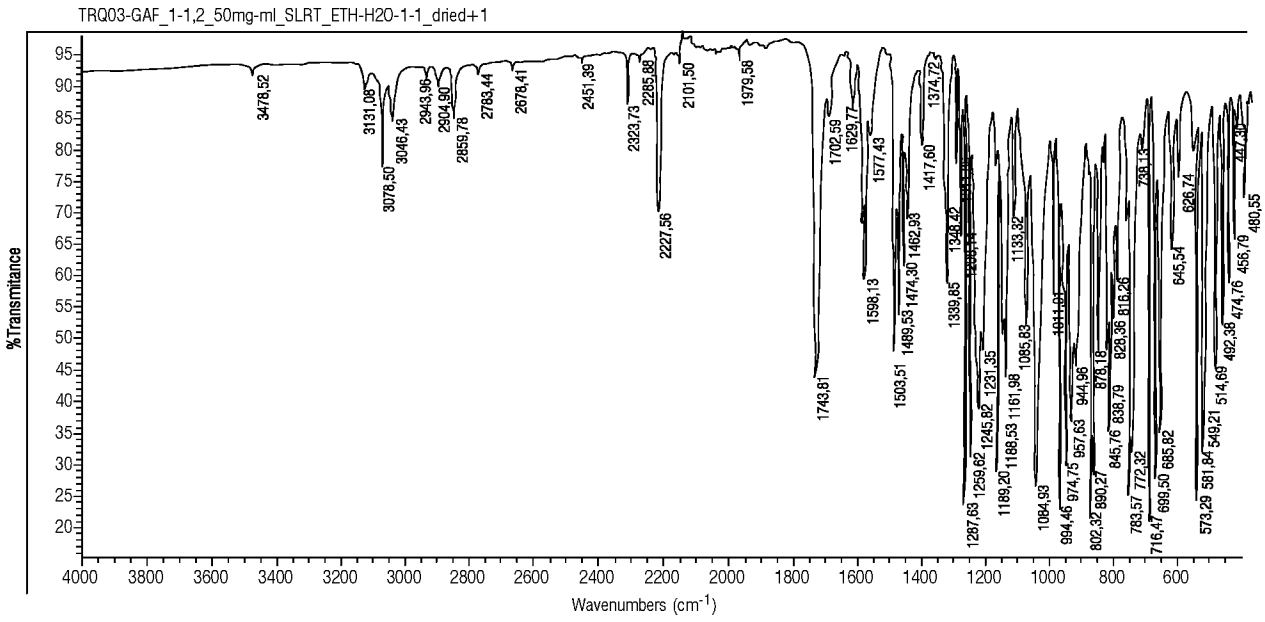
TRQ03-GAF_1-1,2_50mg-ml_SLRT_ETH-H2O-1-1_dried+1
%Transmitance
Wavenumbers (cm-1)
3478,52
3131,08
3078,50
3046,43
2943,96
2904,90
2859,78
2783,44
2678,41
2451,39
2323,73
2285,88
2227,56
2101,50
1979,58
1743,81
1702,59
1629,77
1577,43
1503,51
1489,53
1474,30
1462,93
1417,60
1374,72
1339,85
1259,62
1245,82
1231,35
1189,20
1188,53
1161,98
1133,32
1085,83
1084,93
994,46
974,75
957,63
944,96
890,27
878,18
845,76
838,79
828,36
816,26
783,57
772,32
738,13
716,47
699,50
685,82
645,54
626,74
581,84
573,29
549,21
514,69
492,36
474,76
456,79
447,30
480,55

Fig. 8

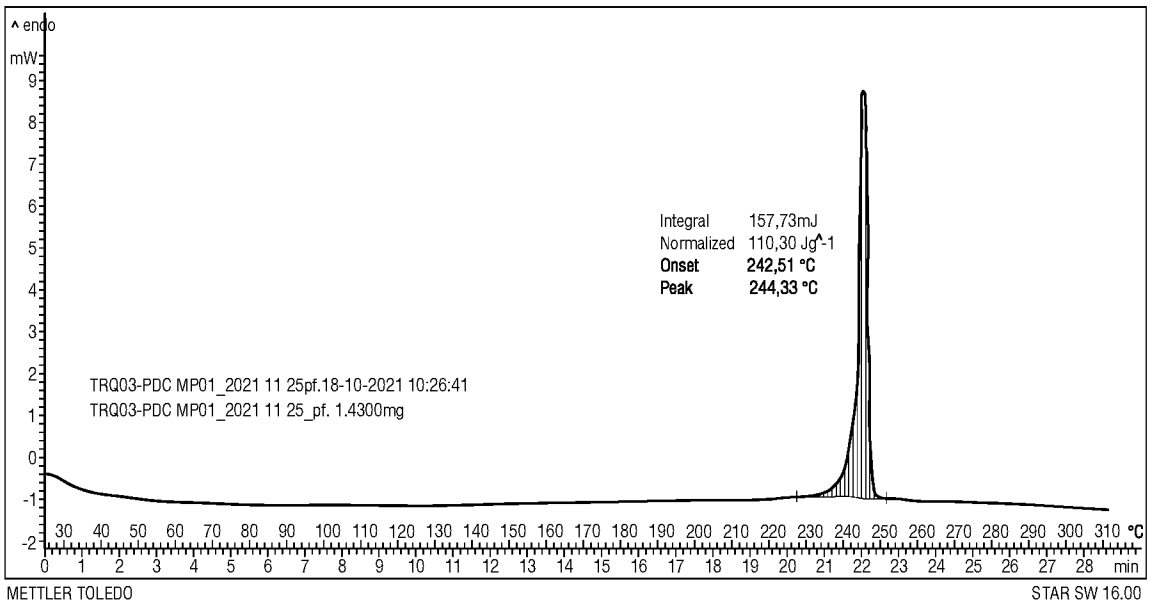
^ endo
mW
Integral 157,73mJ
Normalized 110,30 Jg^-1
Onset 242,51 °C
Peak 244,33 °C
TRQ03-PDC MP01_2021 11 25pf.18-10-2021 10:26:41
TRQ03-PDC MP01_2021 11 25_pf. 1.4300mg
°C
min
METTLER TOLEDO
STAR SW 16.00

Fig. 9

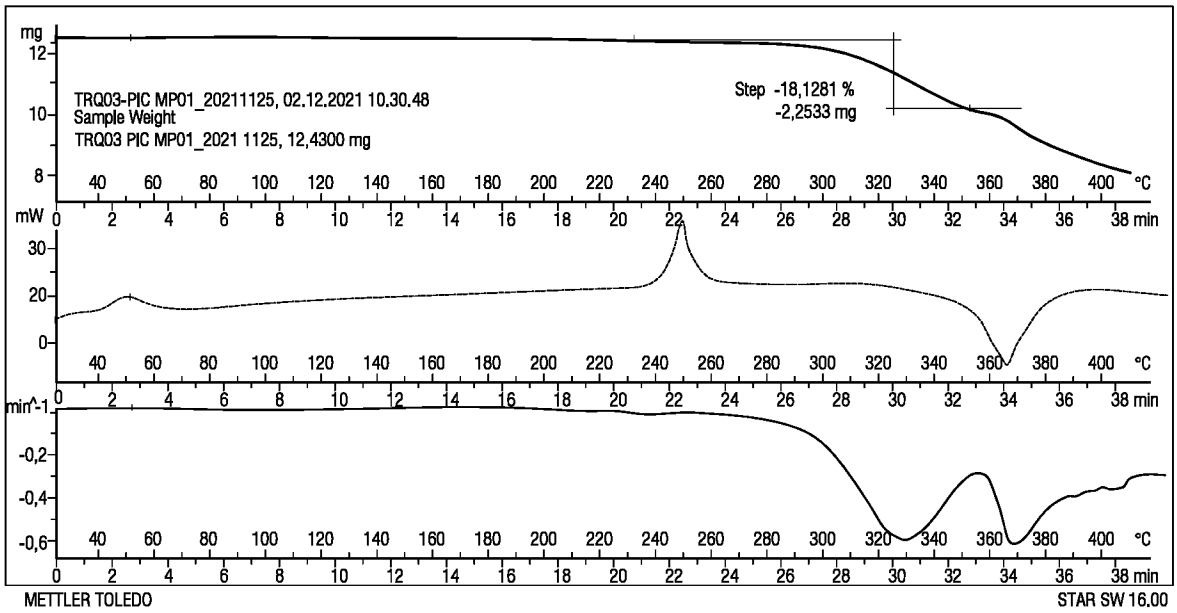
mg
12
10
8
TRQ03-PIC MP01_20211125, 02.12.2021 10.30.48
Sample Weight
TRQ03 PIC MP01_2021 1125, 12,4300 mg
Step -18,1281 %
-2,2533 mg
40 60 80 100 120 140 160 180 200 220 240 260 280 300 320 340 360 380 400 °C
mW
30
20
0
0 2 4 6 8 10 12 14 16 18 20 22 24 26 28 30 32 34 36 38 min
min^-1
-0,2
-0,4
-0,6
METTLER TOLEDO
STAR SW 16.00

Fig. 10

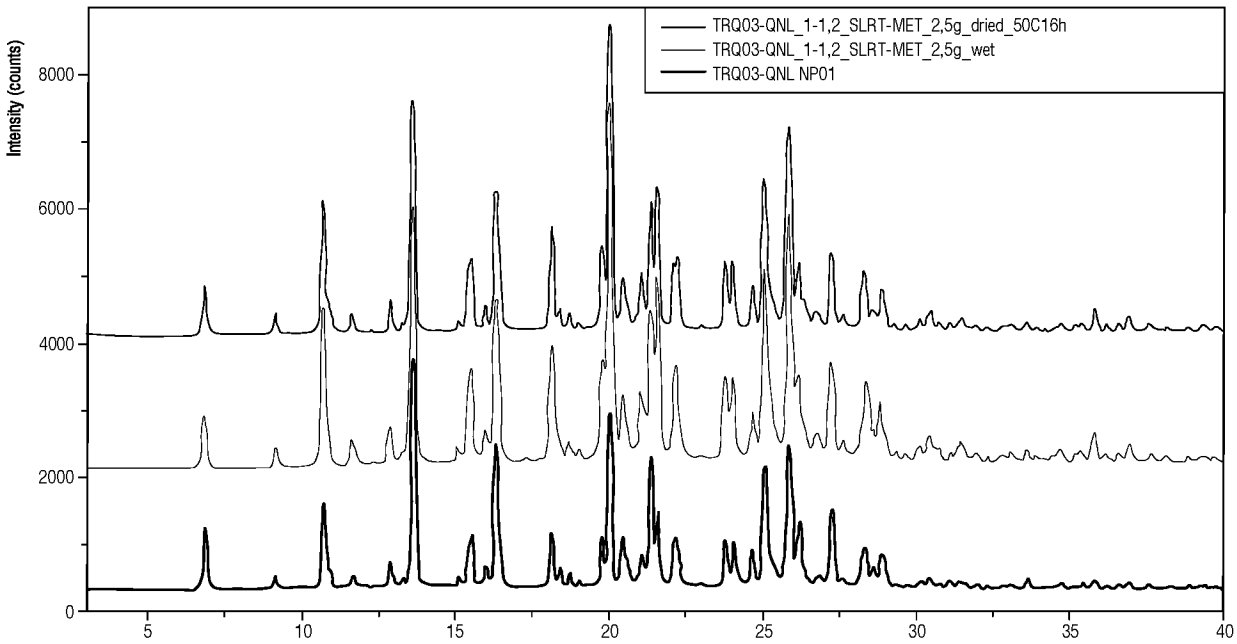
TRQ03-QNL_1-1,2_SLRT-MET_2,5g_dried_50C16h
TRQ03-QNL_1-1,2_SLRT-MET_2,5g_wet
TRQ03-QNL NP01
Intensity (counts)
8000
6000
4000
2000
0
5
10
15
20
25
30
35
40
2θ/°

Fig. 11

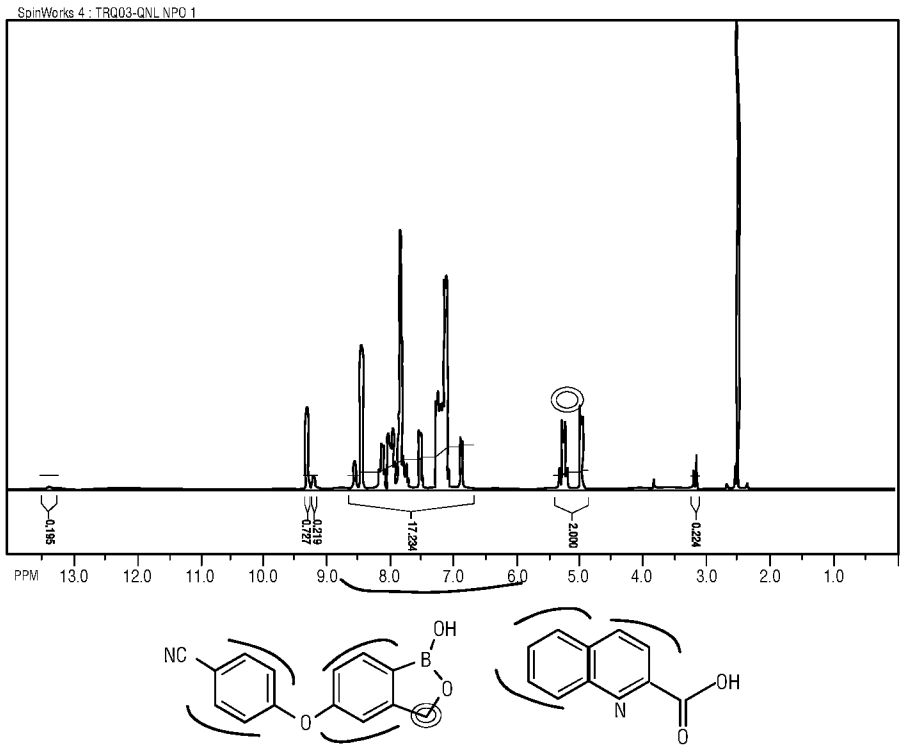
SpinWorks 4 : TRQ03-QNL NPO 1
0.195
0.219
0.227
17.234
2.000
0.224
PPM 13.0 12.0 11.0 10.0 9.0 8.0 7.0 6.0 5.0 4.0 3.0 2.0 1.0
NC
O
B
OH
O
N
OH
O

Fig. 12

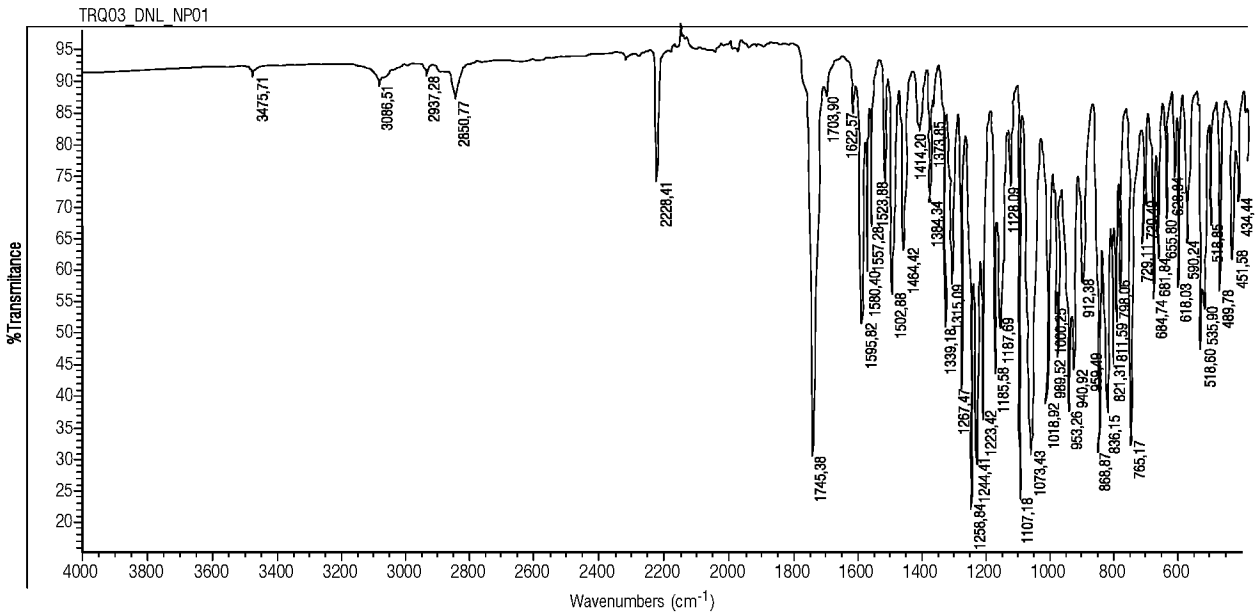
TRQ03_DNL_NP01
%Transmittance
Wavenumbers (cm-1)
3475,71
3086,51
2937,28
2850,77
2228,41
1745,38
1703,90
1622,57
1595,82
1580,40
1557,28
1523,88
1502,88
1464,42
1414,20
1384,34
1339,18
1315,09
1267,47
1258,84
1244,41
1223,42
1185,58
1187,69
1128,09
1107,18
1073,43
1018,92
988,52
953,26
940,92
912,36
868,87
836,15
821,31
811,59
798,06
765,17
729,11
684,74
681,84
655,80
618,03
590,24
535,90
518,60
489,78
451,58
434,44

Fig. 13

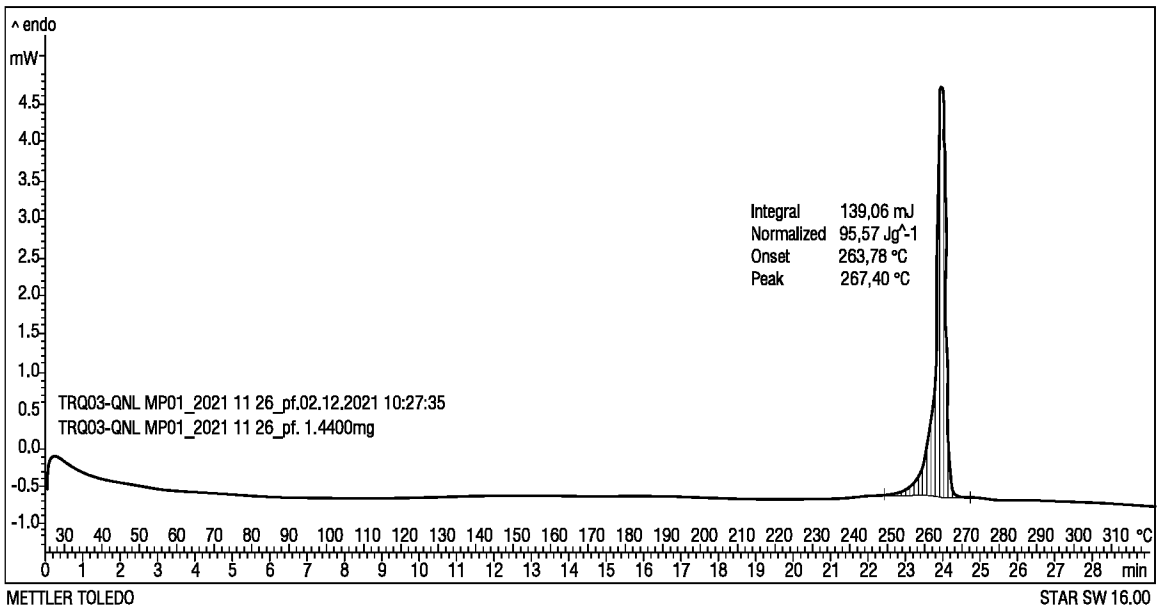
^ endo
mW
4.5
4.0
3.5
3.0
2.5
2.0
1.5
1.0
0.5
0.0
-0.5
-1.0
Integral 139,06 mJ
Normalized 95,57 Jg^-1
Onset 263,78 °C
Peak 267,40 °C
TRQ03-QNL MP01_2021 11 26_pf.02.12.2021 10:27:35
TRQ03-QNL MP01_2021 11 26_pf. 1.4400mg
30 40 50 60 70 80 90 100 110 120 130 140 150 160 170 180 190 200 210 220 230 240 250 260 270 280 290 300 310 °C
0 1 2 3 4 5 6 7 8 9 10 11 12 13 14 15 16 17 18 19 20 21 22 23 24 25 26 27 28 min
METTLER TOLEDO
STAR SW 16.00

Fig. 14

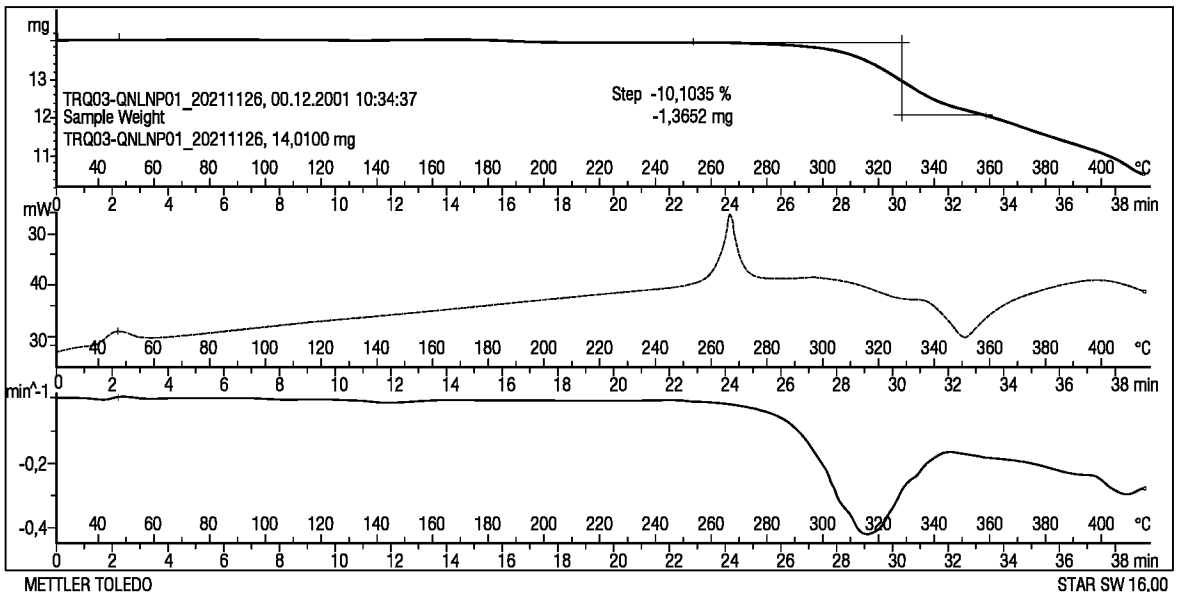
mg
13
12
11
TRQ03-QNLNP01_20211126, 00.12.2001 10:34:37
Sample Weight
TRQ03-QNLNP01_20211126, 14,0100 mg
Step -10,1035 %
-1,3652 mg
40 60 80 100 120 140 160 180 200 220 240 260 280 300 320 340 360 380 400 °C
0 2 4 6 8 10 12 14 16 18 20 22 24 26 28 30 32 34 36 38 min
mW
30
40
30
40 60 80 100 120 140 160 180 200 220 240 260 280 300 320 340 360 380 400 °C
0 2 4 6 8 10 12 14 16 18 20 22 24 26 28 30 32 34 36 38 min
min^-1
-0,2
-0,4
40 60 80 100 120 140 160 180 200 220 240 260 280 300 320 340 360 380 400 °C
0 2 4 6 8 10 12 14 16 18 20 22 24 26 28 30 32 34 36 38 min
METTLER TOLEDO
STAR SW 16.00

Fig. 15

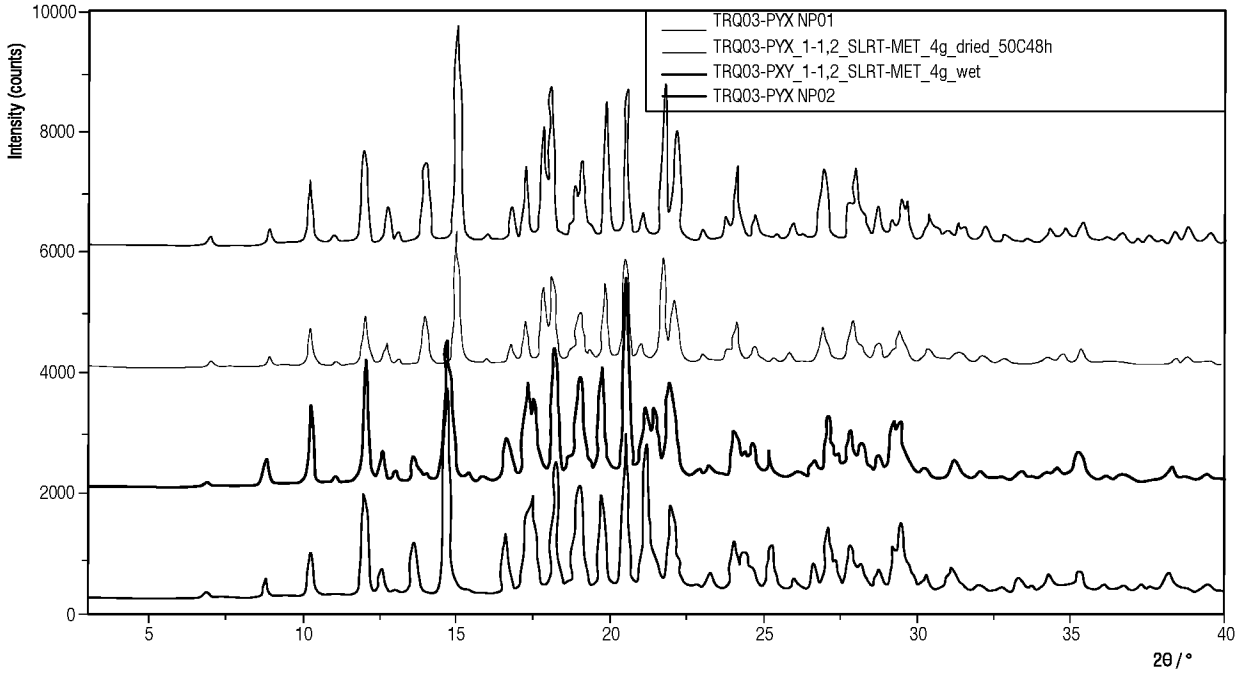
TRQ03-PYX NP01
TRQ03-PYX_1-1,2_SLRT-MET_4g_dried_50C48h
TRQ03-PXY_1-1,2_SLRT-MET_4g_wet
TRQ03-PYX NP02
Intensity (counts)
10000
8000
6000
4000
2000
0
5
10
15
20
25
30
35
40
2θ/°

Fig. 16

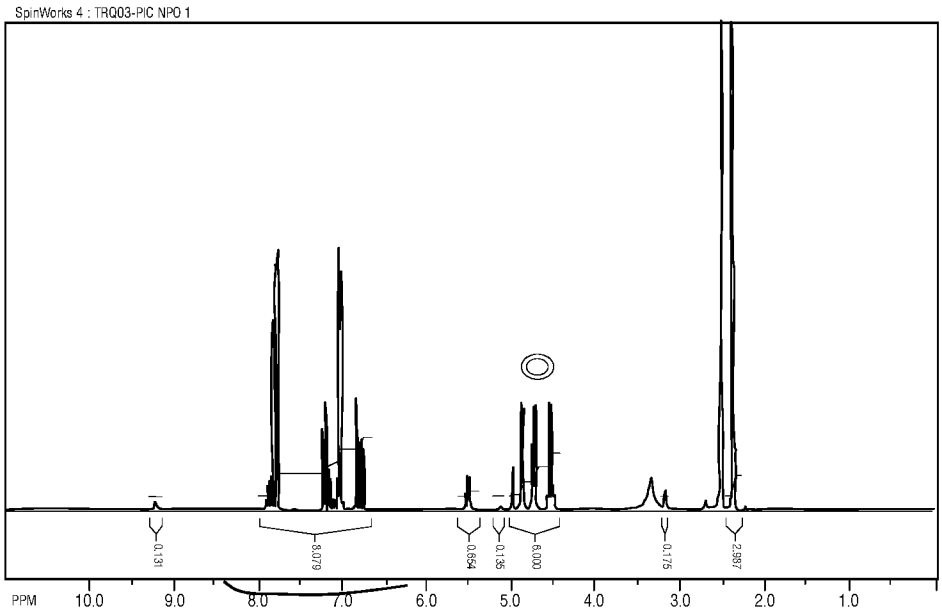
SpinWorks 4 : TRQ03-PIC NPO 1
0.131
8.079
0.654
0.135
8.000
0.175
2.987
PPM
10.0
9.0
8.0
7.0
6.0
5.0
4.0
3.0
2.0
1.0

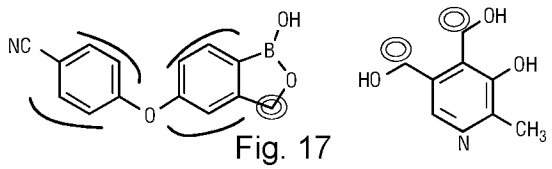
NC
O
B
OH
O
HO
OH
OH
N
CH3

Fig. 17

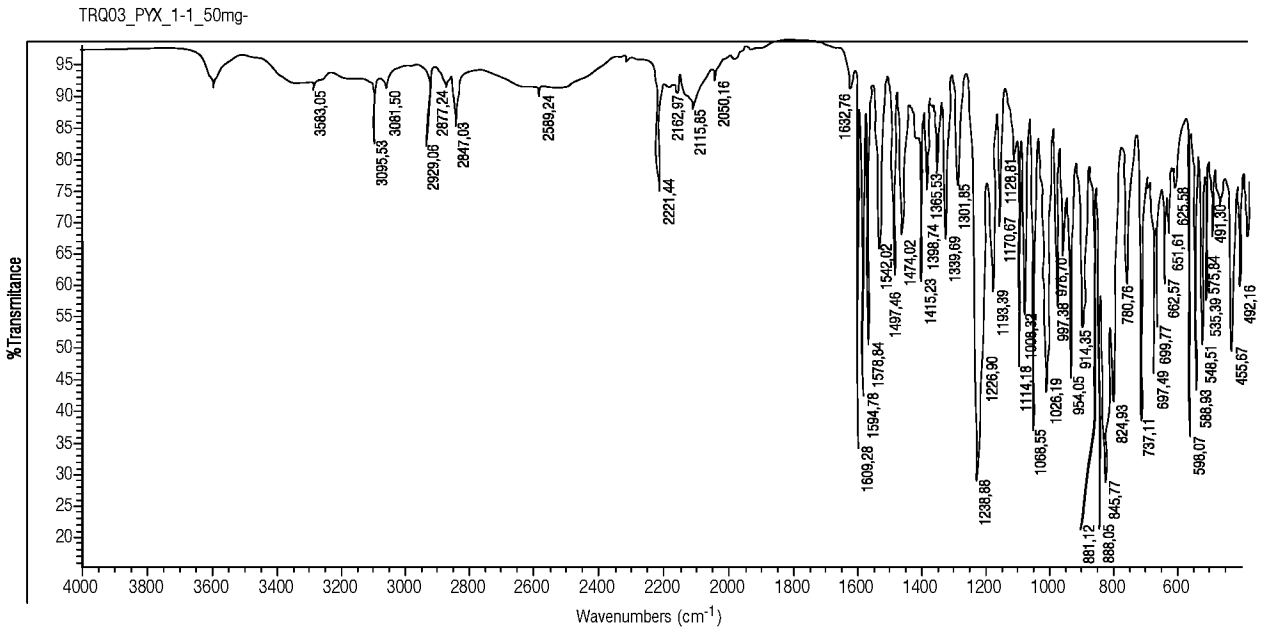
TRQ03_PYX_1-1_50mg-
%Transmitance
Wavenumbers (cm-1)
3583,05
3095,53
3061,50
2929,06
2877,24
2847,03
2589,24
2221,44
2162,97
2115,85
2050,16
1632,76
1609,28
1594,78
1578,84
1542,02
1497,46
1474,02
1415,23
1398,74
1365,53
1339,69
1301,85
1238,88
1226,90
1193,39
1170,67
1128,81
1114,18
1098,32
1068,55
1026,19
997,36
976,70
954,05
914,35
888,05
881,12
845,77
824,93
780,76
737,11
697,49
699,77
662,57
651,61
625,58
598,07
588,93
548,51
535,39
575,84
491,30
492,16
455,67

Fig. 18

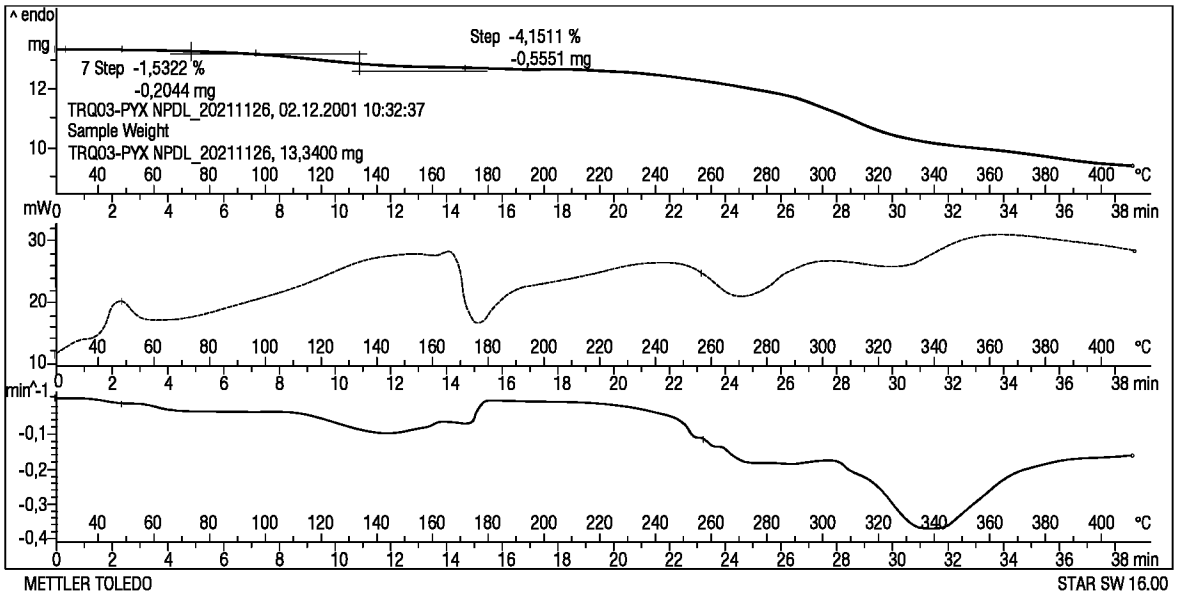
^ endo
mg
12
10
Step -4,1511 %
-0,5551 mg
7 Step -1,5322 %
-0,2044 mg
TRQ03-PYX NPDL_20211126, 02.12.2001 10:32:37
Sample Weight
TRQ03-PYX NPDL_20211126, 13,3400 mg
40 60 80 100 120 140 160 180 200 220 240 260 280 300 320 340 360 380 400 °C
0 2 4 6 8 10 12 14 16 18 20 22 24 26 28 30 32 34 36 38 min
mW
30
20
10
40 60 80 100 120 140 160 180 200 220 240 260 280 300 320 340 360 380 400 °C
0 2 4 6 8 10 12 14 16 18 20 22 24 26 28 30 32 34 36 38 min
min^-1
-0,1
-0,2
-0,3
-0,4
40 60 80 100 120 140 160 180 200 220 240 260 280 300 320 340 360 380 400 °C
0 2 4 6 8 10 12 14 16 18 20 22 24 26 28 30 32 34 36 38 min
METTLER TOLEDO
STAR SW 16.00

Fig. 19

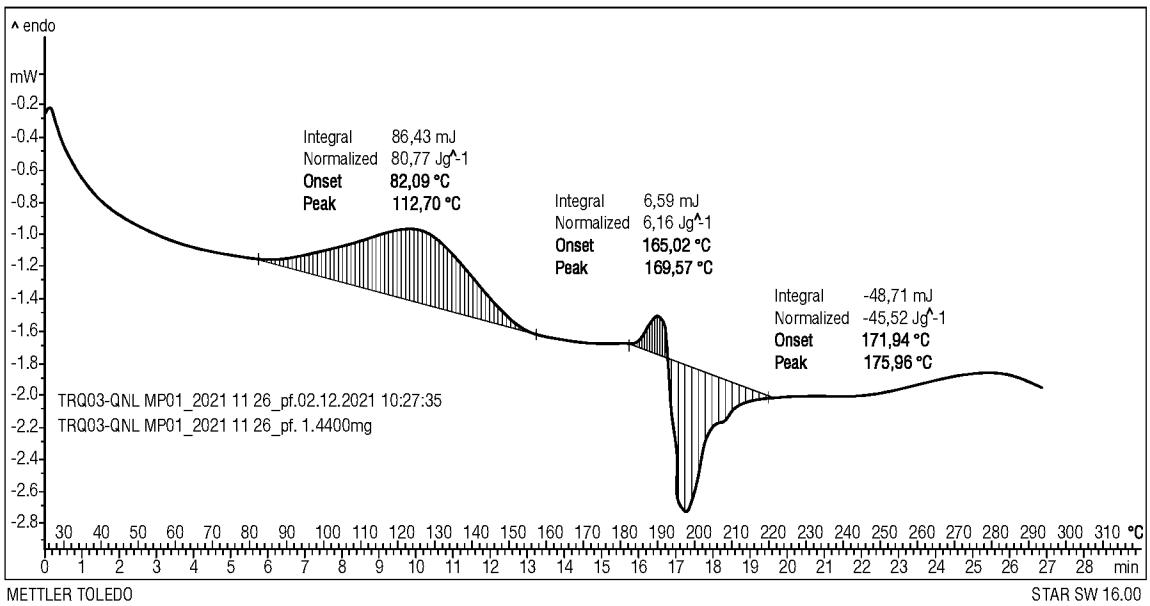
^ endo
mW
-0.2
-0.4
-0.6
-0.8
-1.0
-1.2
-1.4
-1.6
-1.8
-2.0
-2.2
-2.4
-2.6
-2.8
Integral 86,43 mJ
Normalized 80,77 Jg^-1
Onset 82,09 °C
Peak 112,70 °C
Integral 6,59 mJ
Normalized 6,16 Jg^-1
Onset 165,02 °C
Peak 169,57 °C
Integral -48,71 mJ
Normalized -45,52 Jg^-1
Onset 171,94 °C
Peak 175,96 °C
TRQ03-QNL MP01_2021 11 26_pf.02.12.2021 10:27:35
TRQ03-QNL MP01_2021 11 26_pf. 1.4400mg
30 40 50 60 70 80 90 100 110 120 130 140 150 160 170 180 190 200 210 220 230 240 250 260 270 280 290 300 310 °C
0 1 2 3 4 5 6 7 8 9 10 11 12 13 14 15 16 17 18 19 20 21 22 23 24 25 26 27 28 min
METTLER TOLEDO
STAR SW 16.00

Fig. 20

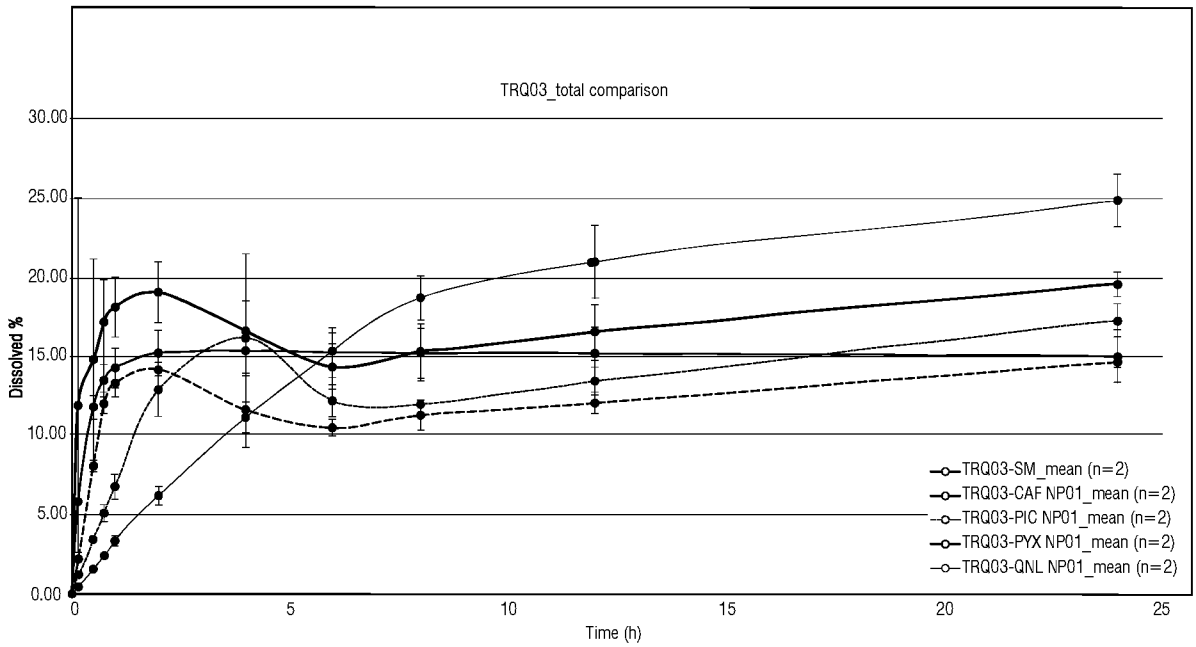
TRQ03_total comparison
30.00
25.00
20.00
15.00
10.00
5.00
0.00
Dissolved %
0
5
10
15
20
25
Time (h)
TRQ03-SM_mean (n=2)
TRQ03-CAF NP01_mean (n=2)
TRQ03-PIC NP01_mean (n=2)
TRQ03-PYX NP01_mean (n=2)
TRQ03-QNL NP01_mean (n=2)

Fig. 21

INTERNATIONAL SEARCH REPORT

International application No.
PCT/IB2023/058612

A. CLASSIFICATION OF SUBJECT MATTER

C07F 5/02 (2006.01)i; C07D 473/12 (2006.01)i; C07D 213/79 (2006.01)i; C07D 215/48 (2006.01)i; C07D 213/67 (2006.01)i
CPC: C07F 5/025; C07D 473/12; C07D 213/79; C07D 215/48; C07D 213/67

According to International Patent Classification (IPC) or to both national classification and IPC

B. FIELDS SEARCHED

Minimum documentation searched (classification system followed by classification symbols)

C07F 5/02; C07D 473/12; C07D 213/79; C07D 215/48; C07D 213/67
CPC: C07F 5/025; C07D 473/12; C07D 213/79; C07D 215/48; C07D 213/67

Documentation searched other than minimum documentation to the extent that such documents are included in the fields searched

Banco de Patentes Brasileiro, Science Direct, Periódicos Capes

Electronic data base consulted during the international search (name of data base and, where practicable, search terms used)

Espacenet, Patentscope, Derwent, Caplus

C. DOCUMENTS CONSIDERED TO BE RELEVANT

Category*	Citation of document, with indication, where appropriate, of the relevant passages	Relevant to claim No.
Y	Gonzalo Campillo-Alvarado, Tighe D. Didden, Shalisa M. Oburn, Dale C. Swenson and Leonard R. MacGillivray, Exploration of Solid Forms of Crisaborole: Crystal Engineering Identifies Polymorphism in Commercial Sources and Facilitates Cocrystal Formation, Cryst. Growth Des. 2018, 18, 4416−4419.	1 - 24
Y	WO 2017193914 A1 (CRYSTAL PHARMACEUTICAL (SUZHOU) CO LTD [CN]) 16 November 2017 (2017-11-16) Whole document	1 - 24
Y	WO 2017203514 A1 (PERRIGO API LTD [IL]) 30 November 2017 (2017-11-30) Whole document	1 - 24
Y	WO 2018013655 A1 (PLIVA HRVATSKA D O O [HR]) 18 January 2018 (2018-01-18) Whole document	1 - 24
Y	WO 2018216032 A1 (MSN LABORATORIES PRIVATE LTD R&D CENTER [IN]) 29 November 2018 (2018-11-29) Whole document	1 - 24

☑ Further documents are listed in the continuation of Box C. ☑ See patent family annex.

* Special categories of cited documents:
"A" document defining the general state of the art which is not considered to be of particular relevance
"D" document cited by the applicant in the international application
"E" earlier application or patent but published on or after the international filing date
"L" document which may throw doubts on priority claim(s) or which is cited to establish the publication date of another citation or other special reason (as specified)
"O" document referring to an oral disclosure, use, exhibition or other means
"P" document published prior to the international filing date but later than the priority date claimed
"T" later document published after the international filing date or priority date and not in conflict with the application but cited to understand the principle or theory underlying the invention
"X" document of particular relevance; the claimed invention cannot be considered novel or cannot be considered to involve an inventive step when the document is taken alone
"Y" document of particular relevance; the claimed invention cannot be considered to involve an inventive step when the document is combined with one or more other such documents, such combination being obvious to a person skilled in the art
"&" document member of the same patent family

Date of the actual completion of the international search	Date of mailing of the international search report
29 September 2023	**10 November 2023**

Name and mailing address of the ISA/BR	Authorized officer
Instituto Nacional da Propriedade Industrial (Brasil) **Rua Mayrink Veiga, 9, 6º andar,** **CEP 20.090-910 Rio de Janeiro – RJ** **Brazil**	**Luiz Eduardo Kaercher**
Telephone No. **(55 21) 3037-3742, 3037-3984**	Telephone No. **552130374528**

C. DOCUMENTS CONSIDERED TO BE RELEVANT

Category*	Citation of document, with indication, where appropriate, of the relevant passages	Relevant to claim No.
Y	WO 2019120637 A1 (OLON SPA [IT]) 27 June 2019 (2019-06-27) Whole document	1 - 24
Y	US 2021002307 A1 (ANACOR PHARMACEUTICALS INC [US]) 07 January 2021 (2021-01-07) Whole document	1 - 24
Y	EP 3521293 A1 (DIPHARMA FRANCIS SRL [IT]) 07 August 2019 (2019-08-07) Whole document	1 - 24
Y	CN 112375093 A (SINOMUNE PHARMACEUTICAL CO LTD) 19 February 2021 (2021-02-19) Whole document	1 - 24
Y	CN 113087733 A (NANJING KEMO BIOMEDICAL CO LTD) 09 July 2021 (2021-07-09) Whole document	1 - 24
Y	IT 201800002347 A1 (DIPHARMA FRANCIS SRL [IT]) 02 August 2019 (2019-08-02) Whole document	1 - 24

INTERNATIONAL SEARCH REPORT
Information on patent family members

International application No.
PCT/IB2023/058612

Patent document cited in search report			Publication date (day/month/year)	Patent family member(s)			Publication date (day/month/year)
WO	2017193914	A1	16 November 2017	AU	2017262235	A1	06 December 2018
				AU	2017262235	B2	19 September 2019
				AU	2017262235	C1	20 August 2020
				BR	112018073017	A2	19 February 2019
				BR	112018073017	B1	14 June 2022
				CA	3023851	A1	16 November 2017
				CA	3023851	C	26 January 2021
				CN	108884111	A	23 November 2018
				EP	3456722	A1	20 March 2019
				EP	3456722	A4	18 December 2019
				IL	262878	A	31 December 2018
				JP	2019520321	A	18 July 2019
				JP	2021167327	A	21 October 2021
				JP	2023116645	A	22 August 2023
				KR	20190005195	A	15 January 2019
				KR	102221472	B1	02 March 2021
				MX	2018013742	A	01 August 2019
				NZ	748385	A	25 March 2022
				RU	2018142490	A	10 June 2020
				RU	2018142490	A3	10 June 2020
				SG	11201809984P	A	28 December 2018
				US	2023234974	A1	27 July 2023
				ZA	201807892	B	30 June 2021
WO	2017203514	A1	30 November 2017	WO	2017203514	A9	18 January 2018
WO	2018013655	A1	18 January 2018	EP	3484895	A1	22 May 2019
				US	2017305936	A1	26 October 2017
WO	2018216032	A1	29 November 2018	US	2020190120	A1	18 June 2020
				US	10865217	B2	15 December 2020
WO	2019120637	A1	27 June 2019	AU	2018389809	A1	18 June 2020
				AU	2018389809	B2	03 August 2023
				CA	3085475	A1	27 June 2019
				CN	111566075	A	21 August 2020
				EP	3728167	A1	28 October 2020
				EP	3728167	B1	01 December 2021
				EP	3851429	A1	21 July 2021
				ES	2903436	T3	01 April 2022
				IL	275381	A	30 July 2020
				US	10329311	B1	25 June 2019
				US	2019194230	A1	27 June 2019
				US	2020407377	A1	31 December 2020
				US	11325922	B2	10 May 2022
				US	2021070781	A1	11 March 2021
US	2021002307	A1	07 January 2021	US	11447506	B2	20 September 2022
EP	3521293	A1	07 August 2019	EP	3521293	B1	07 July 2021
				ES	2881899	T3	30 November 2021
				HR	P20211219	T1	29 October 2021
				US	2019241585	A1	08 August 2019
				US	10597410	B2	24 March 2020
CN	112375093	A	19 February 2021	NONE			

INTERNATIONAL SEARCH REPORT
Information on patent family members

International application No.
PCT/IB2023/058612

Patent document cited in search report	Publication date (day/month/year)	Patent family member(s)	Publication date (day/month/year)
CN 113087733 A	09 July 2021	NONE	
IT 201800002347 A1	02 August 2019	NONE	